CHALMERS
UNIVERSITY OF TECHNOLOGY

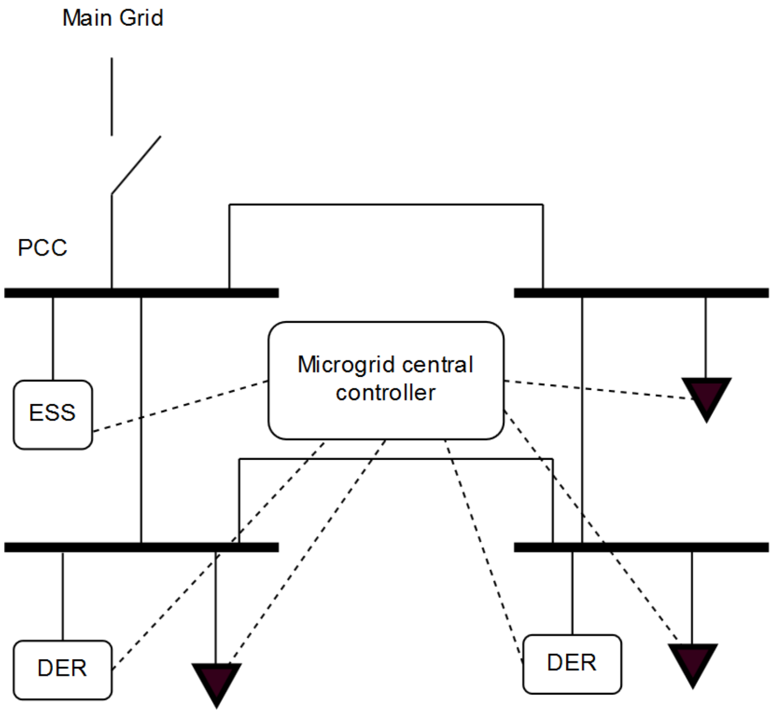

Development of an energy management model for Chalmers' microgrid:

Application for cost-benefit analysis of battery energy storage

Master's thesis in Electric Power Engineering

MARTIN GÖRANSSON
NIKLAS LARSSON

Department of Energy and Environment
CHALMERS UNIVERSITY OF TECHNOLOGY
Gothenburg, Sweden 2016

Master's thesis 2016

Development of an energy management model for Chalmers' microgrid: Application for cost-benefit analysis of battery energy storage

MARTIN GÖRANSSON

NIKLAS LARSSON

CHALMERS
UNIVERSITY OF TECHNOLOGY

Department of Energy and Environment
Division of Electric Power Engineering
Chalmers University of Technology
Gothenburg, Sweden 2016

Development of an energy management model for Chalmers' microgrid
Application for cost-benefit analysis of battery energy storage
Martin Göransson
Niklas Larsson

© Martin Göransson
Niklas Larsson, 2016.

Supervisor and Examiner: Anh Tuan Le, Division of Electric Power Engineering

Department of Energy & Environment
Division of Electric Power Engineering
Chalmers University of Technology
SE-412 96 Gothenburg
Sweden
Telephone +46 31 772 1000

Development of an energy management model for Chalmers' microgrid: Application for cost-benefit analysis of battery energy storage
Niklas Larsson
Martin Göransson
Department of Energy & Environment
Chalmers University of Technology

Abstract

A microgrid is a portion of a larger grid which can be operated independently, thus it is seen as a single entity from the main grid which can be operated in grid connected or island mode. The microgrid consists of distributed energy resources (DER), energy storage system (ESS) and loads which can be controllable. This thesis is a pre-study regarding Chalmers' grid as a microgrid. The aim of this thesis is to evaluate the technical and economical performance of Chalmers' microgrid. In this thesis, a database containing grid data and load profiles for the Chalmers' grid was established. This database was used as input in the developed energy management model (EMM) for the microgrid, which is a planning model used to schedule and optimize own generation, flexible loads and energy storage within the microgrid. A microgrid simulation platform (MSP) was developed containing the EMM in GAMS and data handling in MATLAB enabling simulations with varying input parameters such as ESS capacity and its location.

The MSP is used for benefit-cost analysis of different ESS sizes and locations, and finally for case studies regarding increased amounts of renewable energy (solar PV), island mode operation and vehicle to grid technology (V2G). Results from the analysis show that the total annual cost of electricity can be reduced by 8.43% by including 6 MWh of Li-ion battery storage and increasing the amount of local solar energy to 3 MWp, while also enabling the grid to be operated in island mode for 1 hour periods. With today's battery prices and expected lifetime, investing in a higher amount of solar PVs and a smaller ESS yields the best investment. The case studies show that running the microgrid in island operation is possible, however to do so for a long time requires a large size of ESS. By running part of Chalmers' grid as a microgrid, thus having a higher generation to load ratio, the ESS size could be decreased. With increases in renewable energy capacity at Chalmers, the size of batteries to accomplish island-mode operation is reduced. The V2G technology enables the batteries of the vehicles to act as a distributed ESS. The results show that the benefits gained by including electric vehicles are less than the benefits gained by stationary battery storage. This is due to the vehicles being present within the grid during daytime, thus the batteries cannot be charged during the night when electricity prices are lower. There are economical benefits to be gained from operating Chalmers' grid as a microgrid, however, the investment cost in battery energy storage today is high compared to the benefits gained. Other benefits gained by microgrid operation include enhanced reliability and increased local control.
Keywords: Optimal power flow (OPF), Microgrid, Campus, Energy storage system (ESS), Cost-benefit analysis

Acknowledgements

Firstly, we would like tot thank our supervisor Anh Tuan Le for all his help and support. We would also like to thank Richard Block, Per Löveryd and their colleagues at Akademiska Hus for helping out with measurements and grid data for Chalmers. Finally we would like to thank David Steen for his help and expertise regarding GAMS modeling.

Niklas Larsson & Martin Göransson, Gothenburg, December 2016

Contents

List of Figures

List of Tables

List of Abbreviations

CF	Voltage Correction Factor.
CHP	Combined Heat and Power.
CRF	Capital Recovery Factor.
DER	Distributed Energy Resources.
DNI	Direct Normal Irradiance.
EMM	Energy Management Model.
ESS	Energy Storage System.
EV	Electric Vehicle.
GAMS	General Algebraic Modeling System.
MSP	Microgrid Simulation Platform.
NRMSE	Normalized Root Mean Square Error.
OPF	Optimal Power Flow.
PCC	Point of Common Coupling.
PSS/E	Power System Simulator for Engineering.
PV	Photovoltaics.
RES	Renewable Energy Sources.
SAM	System Advisor Model.
SOC	State of Charge.
V2G	Vehicle to Grid.

List of Symbols

$\boldsymbol{B}$	Susceptance.
$\boldsymbol{C_{ESS}}$	Total cost of energy storage system.
$\boldsymbol{E_{rated}}$	Rated energy capacity of batteries.
$\boldsymbol{Elprice}$	Electricity spot market price.
$\boldsymbol{E}$	Energy.
$\boldsymbol{GC_{CHP}}$	Generation cost for CHP.
$\boldsymbol{G}$	Conductance.
$\boldsymbol{I}$	Current.
$\boldsymbol{PF}$	Penalty factor associated with load curtailment.
$\boldsymbol{P_{CHP}}$	Power output from CHP.
$\boldsymbol{P_{Load,est}}$	Estimated power.
$\boldsymbol{P_{Load,meas}}$	Measured load.
$\boldsymbol{P_{battery}}$	Active power output from batteries.
$\boldsymbol{P_{chr}}$	Charge power from storage.
$\boldsymbol{P_{dis}}$	Discharge power form storage.
$\boldsymbol{P_{fan}}$	Ventilation power.
$\boldsymbol{P_{flex}}$	Flexible active load.
$\boldsymbol{P_{grid}}$	Power from the main grid.
$\boldsymbol{P_{load}}$	Active power load.

$\boldsymbol{P_{pv}}$	Active power from solar PV.
$\boldsymbol{P_{solar,rated}}$	Rated power output for PV.
$\boldsymbol{P_{solar}}$	Normalized power output from PV.
$\boldsymbol{Q_{flex}}$	Flexible reactive load.
$\boldsymbol{SF}$	Scaling factor for load profile.
$\boldsymbol{V}$	Voltage.
$\boldsymbol{\Delta P_{load}}$	Active load regulation.
$\boldsymbol{\Delta Q_{load}}$	Reactive load regulation.
$\boldsymbol{\cos(\phi)}$	Power factor.
$\boldsymbol{\eta_{chr}}$	Charge efficiency.
$\boldsymbol{\eta_{dis}}$	Discharge efficiency.
$\boldsymbol{\theta_{i,j}}$	Voltage angle between bus i and j.
$\boldsymbol{h}$	Hour h.
$\boldsymbol{i}$	Bus i.
$\boldsymbol{m}$	Number of days.

1
Introduction

1.1 Background and Motivations

There are several reasons small-scale Distributed Energy Resources (DER) are being more and more utilized within the distribution grid. A more liberated energy market, higher demand for reliable electric power and new policies regarding environmental friendly power are major factors for this increase [1]. DERs include wind power, solar Photovoltaics (PV), the Electric Vehicle (EV) fleet etc. The distribution grid operator is then faced with a great challenge when trying to operate and control the system. A microgrid aims to help the operator with these issues.

The microgrid consists of locally grouped generation, storage and load within the distribution grid. The local energy resources can be operated to supply the local demand in the most beneficial way. A microgrid can also be disconnected from the distribution grid and be operated independently from the main grid, in the so called island mode. Operating a grid as a microgrid gives more control over the DERs to the microgrid operator and it is easier to include new DERs which might lead to a more economically beneficial operation of the system. The reliability is also increased since the microgrid can be operated independently of the main grid.

There are several challenges when implementing a microgrid. It is important to have a reliable power quality by controlling the voltage and the frequency, which is difficult when many small-scale DERs are used. There is also a need for a sufficient control strategy when the microgrid is operated in island mode in order to keep the system operational. Additional challenges comes in the form of protection requirements and economical challenges [2].

The internal grid at Chalmers has a lot of similarities with a microgrid. It is a clearly defined area with some generation in the form of a Combined Heat and Power (CHP) unit and solar PV. The CHP plant has an electrical power output of maximum 1 MW while the solar PV is rated at 15.7 kW. There are also EVs used at Chalmers which can represent distributed energy storage, although they are not used for this purpose at the moment. Together, the local generation and energy storage could possibly be used to operate part of Chalmers' grid as an autonomous microgrid. The ventilation at Chalmers also has down regulating possibilities, where the total 500 kW of ventilation load can be down regulated by approximately 20% if needed.

The interest to develop microgrids at Chalmers is strong and it is therefore valuable to evaluate how operating Chalmers' grid as a microgrid would benefit the grid owner as well as the grid users. To evaluate and further study the benefits of running Chalmers' grid as a microgrid, there is a need for a model of the internal grid at Chalmers, including the grid data and load profiles for all buses. Alterations in the microgrid, such as increased PV capacity, is also important to evaluate to see which benefits the grid operator could possibly receive.

1.2 Objectives

The objectives of this project include:

- Development of a database for the consumption load profile and grid data for the Chalmers' electrical grid
- Development of an Energy Management Model (EMM).
- Determining the best location and size of battery energy storage for Chalmers' microgrid using a cost-benefit analysis approach based on the EMM.
- Performing a benefit assessment for operating the microgrid for various case studies on PV capacity and EV usage using the developed EMM.

1.3 Specific tasks

In order to achieve the projects' objectives, the thesis is divided into three specific tasks. An overview of these tasks can be seen in Figure 1.1.

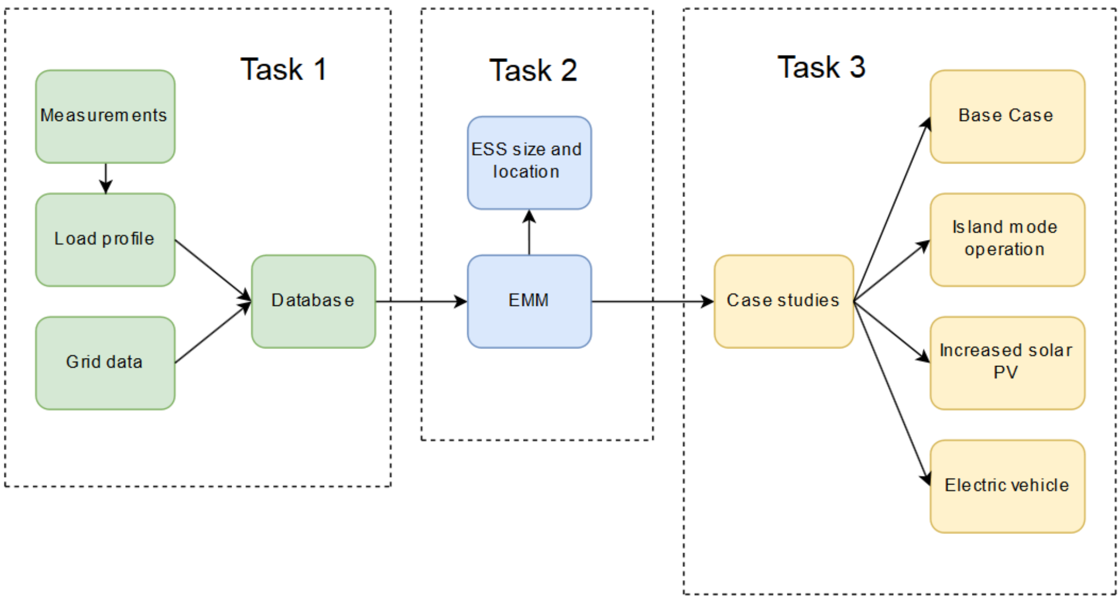

Figure 1.1: Overview of the tasks

Task 1. Load profile and data collection/measurements

Knowledge about the grid and load profiles are necessary to create a model of the internal grid at Chalmers. This needs to be measured in order to acquire data which can be used to obtain accurate and relevant simulations. This task will aim to measure and develop a database of the load profile within Chalmers' grid, as well as data on the internal generation and energy storage units present in the grid.

Task 2. Development of energy management model

In order to simulate the Chalmers' grid a model of it must first be developed. This model will be based on an Optimal Power Flow (OPF) framework which can be used to schedule the local energy resources, which are the flexible loads, local generation and the energy storage. A cost-benefit analysis approach to determine how much energy storage is needed and where it should be placed will be developed. The OPF model, contains constraints such as power flow, flexible load and Energy Storage System (ESS) constraints. The model could be used to evaluate, for example, how the system should be controlled to minimize the cost for the grid owner.

Task 3. Case study using the developed EMM

Several case studies for various configurations of Chalmers' microgrid will be made based on the developed EMM. A base case when the Chalmers' grid is operated as a microgrid will first be evaluated. Island mode operation, an increased amount of solar PV present in the grid and utilizing Vehicle to Grid (V2G) will also be evaluated. These case studies will provide a benefit assessment when running the Chalmers' grid as a microgrid.

1.4 Scope

The project will consider the already existing grid at Chalmers with its currently installed power production (CHP and solar PV). Alterations to the grid will only be considered in the case studies and only in forms of increased generation. The protection system of the grid is assumed to be sufficient and changes in the protection system as a result of the grid being operated as an autonomous microgrid will not be considered. Energy storage in the microgrid will be taken into consideration, that is, location and size of energy storage to achieve a certain amount of time of operation for the Chalmers' grid when disconnected from the main grid. The system is considered in steady state, therefore transient studies will not be conducted. The time resolution of the model will be 1-hour, thus the model will be a planning model since a higher resolution would be necessary for controlling a microgrid.

1.5 Thesis outline

The thesis consists of six chapters including the introduction. The chapters are summarized below:

- Chapter 2 provides a technical background to the project, including previous work on the subject of Microgrids.
- Chapter 3 handles the database development, model formulation and the structure of the Microgrid simulation platform used in the project.

- Chapter 4 explains the cost-benefit analysis which has been performed to find the optimal energy storage from an economical point of view. It also presents results of simulations to obtain the optimal energy storage size and location.
- Chapter 5 handles case studies which have been performed regarding Island mode operation, increased renewable energy generation and implementation of V2G with electric vehicles in the microgrid. The case studies are explained and their results are presented.
- Chapter 6 consists of a conclusion of the thesis and some proposals of future work.

2

Technical background

This chapter aims to discuss the theory behind the microgrid concept, its components and discussions about previous microgrid studies. The chapter also discusses different energy storage possibilities and features of a microgrid.

2.1 The microgrid concept

The microgrid concept revolves around the use of local energy resources, such as generation and storage, to supply a local demand, thus forming a smaller grid within the main grid. This smaller grid is viewed as a subsystem to the main grid with its own control system and is connected at the Point of Common Coupling (PCC). This allows for individual scheduling of local generation and load which in turn can lead to a lower operating cost for the microgrid. An overview of a general microgrid layout is illustrated in Figure 2.1 [3].

A microgrid can be operated both in conjunction with and independently of the main grid provided enough local generation and storage is present to supply the demand. The option to run independently from the main grid, so called island mode, will increase reliability for the microgrid since it can be operational during a fault in the main grid. Microgrids can also disable non essential loads during main grid faults and load peaks in order to prevent local failure and thus keeping the system operational [4].

There are economical aspects to the microgrid concept, in the way that it could potentially be beneficial to transform a small section of the main grid into a microgrid. Since a microgrid is locally controlled, the local energy resources can be scheduled to operate in such a way so the energy cost is minimized. One such energy resource is an ESS, which can be charged during low market price and discharged during high market prices thus lowering the operational cost of the microgrid.

Small scale local energy resources can easily be implemented in a microgrid as long as sufficient control schematics are in place. This can in turn be used to achieve a high renewable penetration by including for example solar and wind power within the microgrid. These types of energy resources can also lower the operating cost since they provide energy from free resources when they are in place [3].

There are several challenges to the microgrid concept which needs to be dealt with before it can be widely implemented. A local control system which makes sure the voltage and frequency fulfill the power quality standards needs to be in place. There are also synchronization issues when connecting to the main grid after being operated in island mode. Another issue with microgrids is the need for ESS which

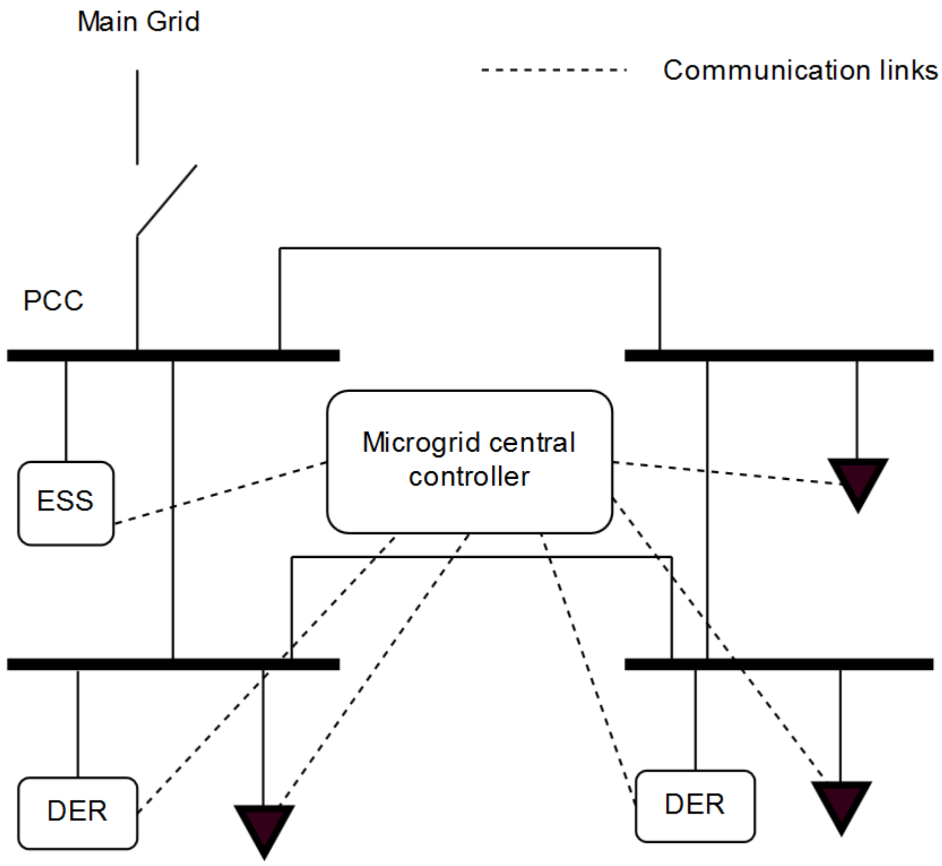

Figure 2.1: A conceptual microgrid with DERs and energy storage

comes with a high investment cost which might exceed the benefits for creating a microgrid, thus making it inefficient from an economical point of view [5].

2.2 Key components of a typical microgrid

This section treats the key components usually present in a microgrid. This includes generation and storage technologies.

2.2.1 Electrical distribution grid

The most key component to a microgrid is having an electrical distribution grid where part of it can be transformed into a microgrid. The microgrid does not include the transmission grid but simply a portion of the distribution grid, where DERs and energy storage can be included to form a microgrid. The distribution grid forms the role of distributing power to the end customers, for example feeding industries or facilities.

2.2.2 Distributed power generation

There are several different methods to generate power within the power grid. However, only small scale energy resources is appropriate in a microgrid since the local energy demand usually is small in a microgrid. At Chalmers there is currently a CHP-plant and solar PV installed which are both suitable energy resources in a microgrid.

2.2.2.1 Combined heat and power

Combined heat and power is a method of creating heat as well as electric power within the same plant. CHP systems deliver the majority of its output energy as heat with a smaller portion of electrical energy. This can be accomplished by the utilization of a stream turbine where high pressured steam is forced through a turbine which is connected to a synchronous generator. The generator produces the electrical part of the generated power. The heat is extracted in the form of hot water which comes from low-pressure steam utilization in heat exchangers [6]. This process is illustrated in Figure 2.2.

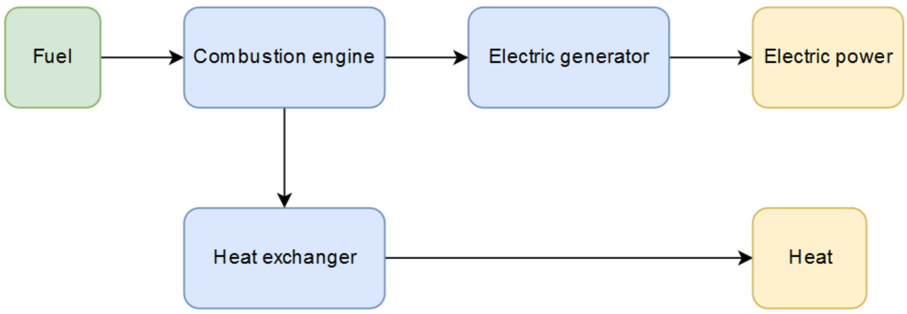

Figure 2.2: Working principle of CHP

2.2.2.2 Solar Photovoltaics generation

Photovoltaics technology, or solar cells, can be used to generate electricity from solar irradiation. Since solar cells are possible to mount on top of buildings they could be a suitable technology for microgrids where the area available for generation units could be limited. Another benefit of solar PV is the fact that it can be easily scaled by simply increasing the amount of solar cells to obtain the desired power generation. The general working principle of solar photovoltaics is shown in Figure 2.3. If there are any DC loads such as battery storage, the energy from the solar panels can be directly transferred to the battery storage instead of going through the conversion process shown in 2.3 to supply the AC loads.

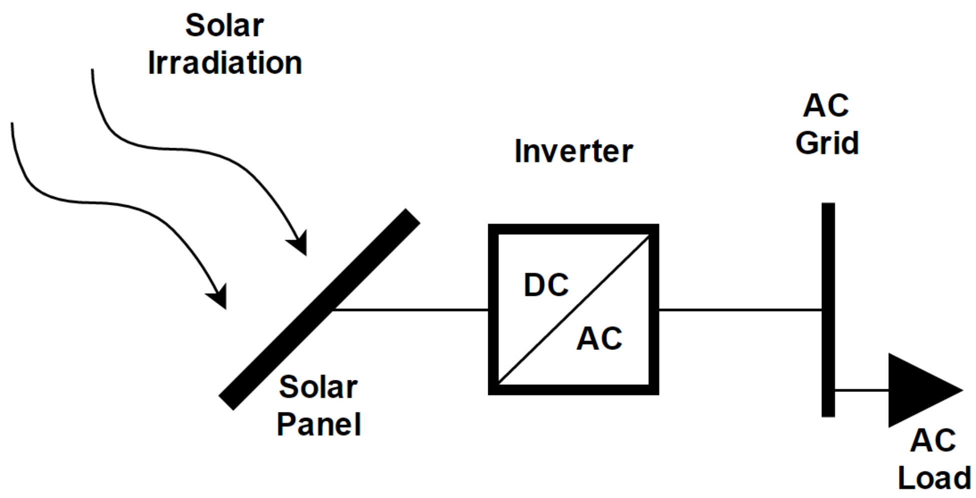

Figure 2.3: Working principle of solar PV

2.2.2.3 Wind power

Wind power is a renewable energy resource which can be implemented in a microgrid. In a similar matter as solar power, the generation is dependent on weather conditions and can therefore not be relied on to produce a constant power output. Wind power comes with a downside of creating noise which can be disturbing depending on the location of the microgrid. Although Wind power is currently not included in Chalmers grid it is a possible DER to be used within microgrids.

2.2.3 Energy storage

Energy storage is an important part of the microgrid system. It serves several different purposes such as frequency regulation, reliability improvement, peak power shaving and energy management applications leading to a lower cost for the system. The main purpose of energy storage is different depending on the conditions the microgrid is operated under. In a microgrid with high amounts of Renewable Energy Sources (RES), that are unreliable by nature, the energy storage systems are mainly used to improve the reliability of the system by storing excess power when available and supplying it when the power production is low.
In a microgrid without sufficient generation to operate independently, the storage can be used to achieve operation in island mode for a certain amount of time. It can also be used for peak power shaving in all types of microgrids making the system more economical to operate. Energy storage may also simplify black starting of the microgrid since the energy stored can be supplied to the grid during this event [7].
The energy storage can be constructed in either an aggregated manner or as a distributed energy storage system. The difference between the two is that the aggregated ESS has all the storage placed at the microgrid terminal so that the power flow to the microgrid can be controlled at the point of common coupling (PCC) while in a distributed ESS the storage is spread out between different generation units within the microgrid. The distributed ESS enables optimization of storage depending on generation type.

2.2.3.1 Batteries

Batteries are a well known way of storing electrical energy and has been used for a long time. There are different types of batteries, such as Lead-acid, Sodium-Sulfur (NaS), Nickel-Cadmium (NiCd), Nickel-MetalHydride (NiMh) and Lithium-ion (Li-ion) batteries. The efficiency of battery storage can be estimated to 60-80% depending on type and depth of discharge. There are several aspects to factor in when choosing a battery type, such as price, energy density, power density and how environmental friendly the batteries are [7]. The advantages of li-ion batteries comes in the form of high power and energy density but with the drawback of having a relatively high cost [8]. When looking at battery storage for microgrids, it is shown that the discount rate used for economical analysis influences which battery type is the most suitable. For discount rates above 4% li-ion is shown to be the most cost effective battery storage alternative [9]. The investment cost for batteries has declined by 8% annually and was around 300$/kWh in 2015 [10]. Since the EV industry is growing, the need for better and cheaper batteries is growing with it. For EVs to be cost competitive with the classical combustion vehicles the battery cost need to be lower than 150 $/kWh [10]. Out of all commercially availible battery storage technologies, the Li-ion battery is the best choice for high power and high energy applications [3].

2.2.3.2 Vehicle to grid (V2G)

The concept of V2G is based on the energy stored in the EVs. Electric vehicles can be of different types, such as plug in hybrid EV, fuel cell EVs and battery EVs. For hybrid EVs and battery EVs, the energy is stored in batteries, and for battery EVs a connection to the grid is required for charging. Electric vehicles that are grid connected enables the energy stored in the batteries to be supplied to the grid. Vehicle to grid is thereby a type of battery energy storage which can be used for microgrid applications [11].
With an increasing amount of EVs, possibilities in generation are increasing. For the USA, assuming a car fleet consisting of 25 % EVs the total power generation can be estimated to 660 GW. It is shown that the vehicles are used about 4 % of the time on average, meaning that the energy stored within the vehicles can possibly be used for other purposes such as V2G [12].

2.2.3.3 Flywheel

Flywheel energy storage is based on storing energy as kinetic energy within a flywheel which can then be converted to electrical energy though an electric machine when needed. Flywheels have a very short response time and are capable of delivering high power levels. This makes them useful for protecting critical loads since they are able to respond quickly and keep the system operating until other forms of generation can be online. The lifetime of a flywheel is long compared to batteries and is almost independent of the charge/discharge pattern. This allows for many charge cycles and there is no need for periodic maintenance [13].
The drawbacks with flywheels as a type of energy storage are the storage capability,

large size and high standby losses. This makes flywheels unsuitable for long time energy storage [7].
In today's grid, flywheels are used to protect critical loads, such as hospitals, from system failures. They are able to prevent failures without additional generation in most cases as 97% of all AC outages lasts for less than 3 seconds. However, for longer failures other energy sources need to be activated in order to keep the system operational [14].

2.2.3.4 Supercapacitors

Supercapacitors (also know as ultracapacitors) operate under the same principles as regular capacitors in that they store energy by separating charge. However, supercapacitors have a much higher capacitance for its size compared to regular capacitors. By separating the charge, the energy storage is made without the chemical process required by batteries thus supercapacitors can achieve a very fast response time [7].
Supercapacitors have a high power density comparing to batteries and can thus charge and discharge quickly. However, batteries can store more energy than a supercapcitor and also have a lower self-discharge rate when storing energy over longer time periods [7], [15].
It has been shown that supercapacitors have a high cycle lifetime, typically hundreds of thousands cycles, for a 100 % discharge depth. These advantages makes supercapacitors ideal when dealing with frequency control, transients and short-term storage [15].

2.3 Features of microgrids

The benefits of running a section of a grid as a microgrid come in different forms. For instance, one can schedule the local energy resources in such a way that the operating cost is minimized. This includes scheduling the use of ESS and controllable loads. Other benefits comes in the form of control over the grid and what energy resources that can be included.

2.3.1 Demand response

The principle of demand response is based on evening out the hourly demand of power. By shifting the demand from the demand peaks to off-peaks the total cost of energy can be lowered. This can be done by moving the controllable loads in time to when the electricity price is lower thus reducing the total cost. Demand response can also be used in emergencies, for example in hospitals, to lower the total load by only operating the essential loads and thus keeping the system operational [16]. For industrial users the price paid for electricity is also determined partly by the peak demand of the facility, thus lowering the peak demand can further decrease the cost [17].
In a grid with a high renewable penetration it could be beneficial to shift demand to hours where the generation is high. However, this might increase the peak demand which requires a higher capability system [16].

One way of implementing demand response in a local power system is to include an ESS unit. The grid can then use the ESS as a generating unit when the demand is high thus lowering the total power provided by the main grid. The ESS will then recharge when the demand is low in order to be ready for use during the next demand peak.

2.3.2 Energy management system in microgrids

An energy management system (EMS) is a software which controls the DERs, loads and their scheduling within the microgrid. Knowledge about grid states and market prices are necessary to schedule generation and load, therefore communication between the EMS and generation and load units are necessary. The aim of the energy management system is to optimize the controls of load, generation units and power flow [18]. This means that scheduling of units within the microgrid can be considered an optimization problem, where the objective can be to minimize the total energy cost for example. The EMS is located within the microgrid central control (MCC) as shown in figure 2.1.

2.4 Previous Work

This section discusses some previous work on the subject of microgrids, as well as experimental microgrids that have been tested.

2.4.1 Sizing of Energy Storage Systems

Sizing of energy storage systems designed for microgrid applications is relevant from a cost-benefit point of view. Determining the optimal size of the energy storage includes considering the minimal size of the energy storage. The minimum size of the storage depends on the application, but for island mode microgrids, the possibility of running the microgrid independently must be considered. With the objective of minimizing the total cost for an island mode microgrid and maximizing the total benefits for a grid-connected microgrid a study was made resulting in two models with the aim of finding a solution to both objective functions [19]. These methods aims to find the optimal size for both island mode and grid connected operation. The solver used was a MILP solver and the method aims to evaluate different storage sizes between a chosen minimum and maximum size and find which the most beneficial size is. The study shows that an optimal solution to sizing of energy storage exists where the solution is different for grid-connected and island mode microgrids. The study shows that the total cost could be reduced by 8.64% per day for the island mode microgrid [19].
Another method of finding the optimal size of energy storage could be to utilize genetic algorithm (GA) which has been used for unit commitment and other power system problems. GA is based on natural evolution and natural selection, and there is a probabilistic approach to the solution. The benefits of using GA is that it provides several solutions, and that the iterative search of an optimal solution is conducted over a population of solutions rather than one [20]. There is also a

method called multiobjective particle swarm optimization (MOPSO) which can be used to solve problems including several objectives [3].

2.4.2 Experimental Microgrids

Testing of the microgrid technology has been conducted in several places over the world, where evaluation of its functionality has been done.

2.4.2.1 CERTS testbed US

The CERTS testbed was built near Columbus Ohio US, where the microgrid concept was tested at a full scale with 3x60 kW generation units, each with an energy storage located at its DC bus. The aim of the project was to test the possibility of a smooth transition between grid-connected and island mode, having a reliable protection system and finally a stable system with regards to voltage and frequency in both operation modes. The testing was found to fulfill all set goals regarding power quality standards and the protection system and controls were found to be functioning according to the set goals [21], [22].

2.4.2.2 University of Texas at Arlington microgrid testbed

The university of Texas at Arlington have developed and constructed a microgrid testbed used for research purposes. It consists of three different microgrids placed in a ring layout which allows them to operate separately or together with each other. This allows for simulations on how microgrids can help support other microgrids and thus increasing the reliability of the local power system.
The microgrids consists of solar PV, wind turbines and an ESS. There is also a fuel cell installed in one of the three microgrids and a diesel generator located at the PCC. Each grid is equipped with a flexible load and can further be equipped with conventional loads if deems necessary [23].

2.4.2.3 Microgrid design considerations for Eindhoven University of Technology campus

The transitioning of a university campus grid into a microgrid was considered, where the goal was to propose a design of said microgrid [24]. The consumption of the campus grid was 52 GWh excluding the natural gas consumption of 79 GWh. There was also an already existing thermal energy storage of 20 MW_t which in the thesis is assumed to be increased to 30 MW_t. There is also a planned installation of 10.5 MW_p of solar PV to supply the electrical load at the campus. It is concluded that the RES are producing a power surplus for 220 hours of the year, meaning that this surplus could be exported or stored within the microgrid. Both mobile storage in the form of vehicles and battery storage are also considered within the grid for simulations. The battery storage is assumed to consist of Li-ion batteries with a cost of 500 €/MWh, and a lifetime of 15 years. To ensure the lifetime the State of Charge (SOC) is limited between 0.2 and 0.8. Simulations show that it is only beneficial to include battery storage for limited sizes. It is concluded that battery storage is not beneficial with the investment cost and electricity prices used from 2014. However, with higher electricity prices and cheaper batteries the battery storage is considered to have future potential [24].

2.4.3 Economic analysis of microgrid including EVs

A study from 2011 was conducted regarding the economic benefits of a microgrid including EVs as part of its generation [25]. The study was conducted by simulations using particle swarm optimization which is an iterative optimization method, to schedule the unit commitment within the microgrid. The power flow is bidirectional in the study meaning that the EVs are used for both injecting and taking power from the microgrid. The microgrid studied has an electrical demand of 5.9 GWh/year and a peak demand of 950 kW. The control strategy of EVs is based on generation excess or deficit. When the total generation within the microgrid is greater than the load, the energy is stored within the batteries of EVs and when the generation is less, the batteries of the EVs is used to inject power to the microgrid. The electric vehicles are assumed to have a SOC of 73% when owners arrive at the office. The SOC is limited to not go below 33% during the day. By the proposed contract the microgrid owner and the car owners share the benefits obtained by including EVs in the microgrid. The operational cost of the grid is shown to decrease by 5.02% which is the benefit seen by the grid owner. The car owners get their benefit from a connection payment which is suited to compensate for battery degradation. Battery degradation is increased due to the charging cycles taking place within the microgrid. The study concludes that it is beneficial for both car owners and microgrid operator to include EVs as a part of the microgrid [25].

2.4.4 AC and DC microgrids

Since the main grids around the world are dominated by an AC infrastructure it is easy to implement AC in the microgrids. As more and more power sources that generate DC power are utilized, DC microgrids become more and more attractive. However, the DC technology needs to mature before it can be used as a reliable power system [26].

2.4.4.1 DC microgrids

The reasons why DC microgrids could be a valid option to AC microgrids are several. Many of the customer loads of today are DC powered, and the increase in renewable energy sources is another reason why DC microgrid could be viable. Solar PV and fuel cells are naturally producing DC power, thus it is more efficient to utilize them in a DC grid. Regarding other RESs such as wind turbines, they are often connected to the AC grid via a DC-link, thus by cutting out the conversion stage the efficiency could be increased [27]. There are also challenges associated with DC microgrids, such as protection. It is challenging to construct a protection system for DC since there is no natural zero crossing in DC current [27].

2.4.4.2 AC microgrids

The more conventional AC grid is dominant as of today due to its efficient transformations in voltage level, and also due to fossil fueled generation being well suited for AC [28]. Since a microgrid is often aimed towards including RES, these need to be connected to the grid. Solar PV is naturally producing DC current thus conversion is needed in order to connect them to an AC grid. On the other hand, with increasing amounts of local RES the need for long transmission lines could be reduced in the future [28]. Protection systems can easily be adapted from todays AC grid standards into a microgrid. The case is the same regarding frequency and voltage control, thus making the transition somewhat simple [29].

2.4.4.3 Hybrid microgrid

A study on a hybrid AC/DC microgrid was made in 2011 [28]. This study proposes the use of a AC/DC microgrid to minimize the AC to DC transformations in the grid. An investigation on a hypothetical microgrid consisting of 40 kW PV connected to the DC side, 50 kW wind connected to the AC side and a variable load of 20-40 kW connected on both sides of the microgrid. The study evaluates the stability of the microgrid in both grid connected and island mode operation.
It is concluded that the hybrid AC/DC microgrid proposed offers satisfactory stability both when operated in grid connected and island mode. However, due to the AC infrastructure of the main grids, it is difficult to apply a AC/DC microgrid in today's society [28].

3
Chalmers' grid database and model developments

This chapter describes how the database for the Chalmers' electrical grid and the microgrid simulation platform are developed. The database consists of network data, which was provided by Akademiska Hus, and load data which was taken from different measurements to create load profiles for the grid. These load profiles are then used as input in the EMM which was developed using General Algebraic Modeling System (GAMS) software. The objective of the EMM is to minimize the total energy cost of the system and it is solved with constraints such as power flow equations, network constraints and ESS constraints. The simulated results are then validated by comparing acquired voltages from the grid model to values taken from PSS/E software.

3.1 Database development

A database has been developed consisting of load profiles of the Chalmers grid, grid and generation data. The 12 kV chalmers grid is presented in figure 3.1, however the loads connected to each transformer in the grid were unknown hence a database with this information needed to be developed.
The system consists of of 22 buses of which 17 are load buses. Connection to the main grid is located at bus 07:8 and the CHP plant is located at bus 07:8.1.1, both within the building Kraftcentral. There is also solar PV located at bus 07:8.1.1 not shown in the single line diagram. A backup connection to the main grid is connected to bus 07:35, however, this bus is normally disconnected and is therefore not used in any simulations.

3.1.1 Load Data

In order to create a database of the different loads within the Chalmers grid three different methods to collect data have been used. These are own measurements at a substation, the energy usage in all the buildings measured by Akademiska hus, responsible for the power grid at Chalmers, and current measurements taken from Microscada, also provided by Akademiska hus. By combining these measurements, an accurate load distribution have been created.
Akademiska hus provided a database with the energy consumption within each building for each hour of the day for 2015. This database gives a picture of how

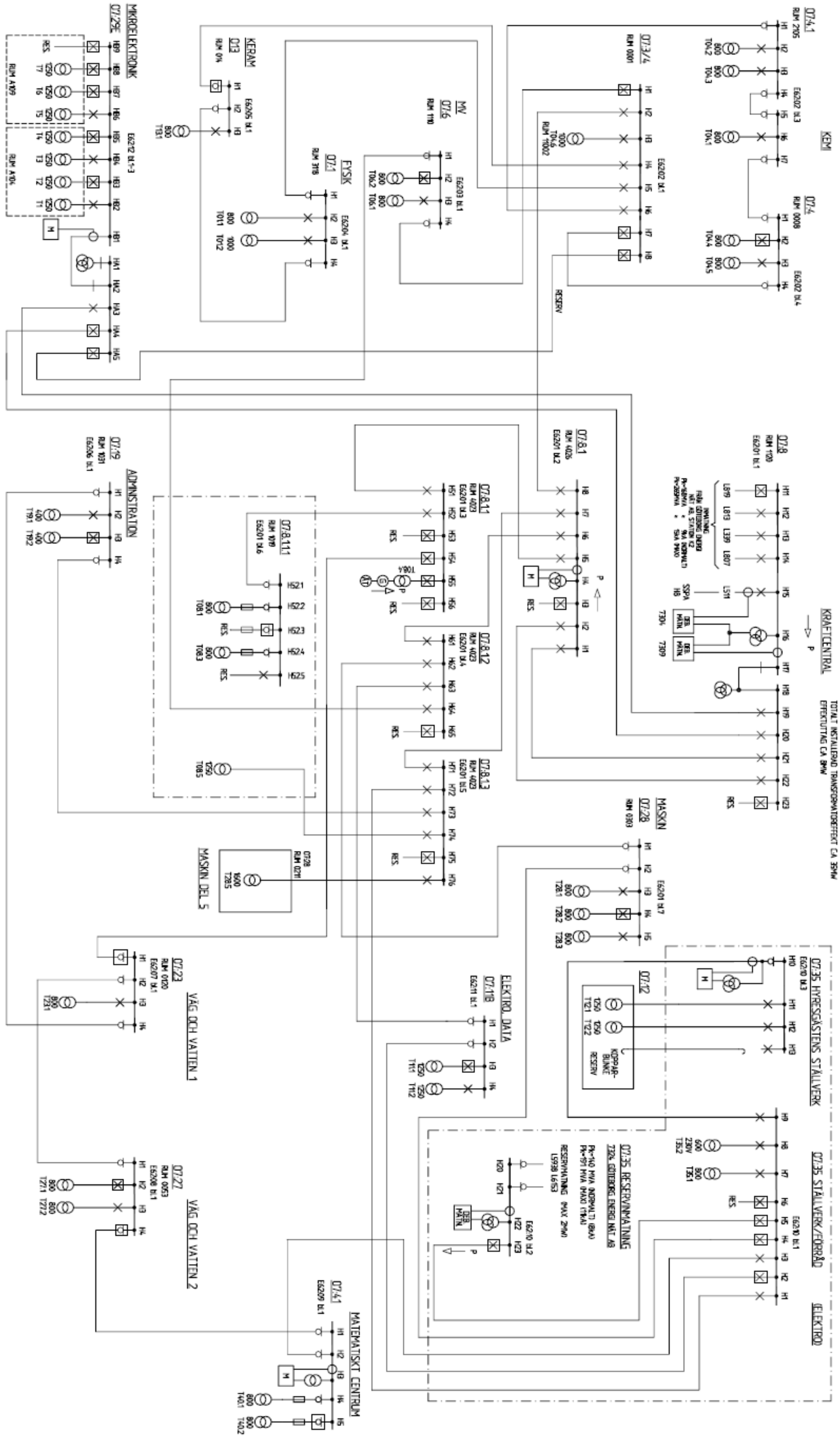

Figure 3.1: 12 kV grid at Chalmers.

the energy demand varies during the day but since not all buildings have their own substations, these values can not readily be inserted into the model. Therefore currents from Microscada are included to construct the load profiles.
Microscada is the software used to monitor the grid within Chalmers and can also be used to monitor the currents within the system. These currents can then be used to calculate the power demand at the substations within the system. However, not all currents are being measured so complementary data has been taken from Akademiska hus database. By comparing the energy consumption data over the year, a scaling factor is determined which is then used to extend the 24-hour load profile to be valid for an entire year. The methodology of constructing the load profiles is shown in Figure 3.2.

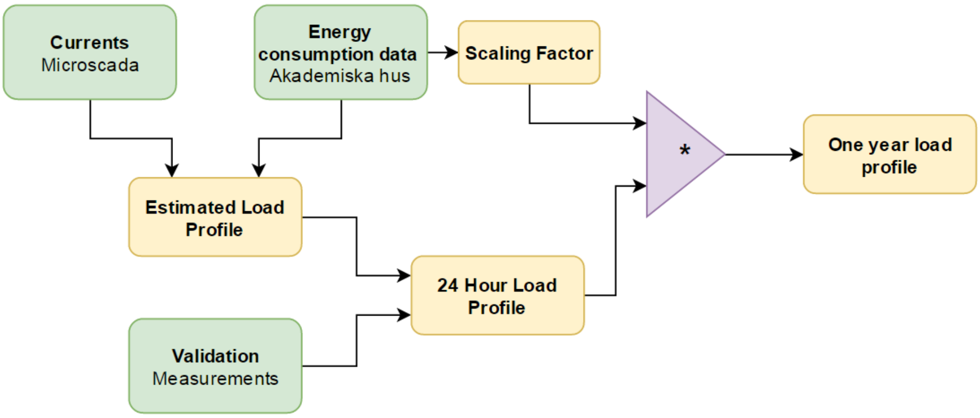

Figure 3.2: Load profile methodology flowchart

The estimated load power, $P_{Load,est}$, for each node i in the grid at every hour h is expressed in Equation 3.1. The voltage V is assumed to be 1 p.u, the load power factor $\cos(\phi)$ is assumed to 0.98 and the current I is taken from Microscada.

$$P_{Load,est}(i,h) = \sqrt{3}|V(i,h)||I(i,h)|cos(\phi) \tag{3.1}$$

3.1.2 Measurements

Measurements have been conducted in substation 07:11B located in the EDIT-building. The voltage, current, power output and power factor have been monitored for half a day between 07:00 and 17:00. These measured values are then used to validate and improve the load profile. By comparing the load profile obtained by the estimation, $P_{Load,est}$, and the actual measured values, $P_{Load,meas}$, the Normalized Root Mean Square Error (NRMSE) ,as described by Equation 3.2, can be calculated.

$$NRMSE = \frac{\sqrt{\frac{1}{n}\sum_{h=1}^{n}(P_{Load,meas}(h) - P_{Load,est}(h))^2}}{\overline{P}_{Load,meas}} \tag{3.2}$$

The voltage is measured which in the estimated value of the load is assumed to 1 p.u. By defining a Voltage Correction Factor (CF) as described in Equation 3.3 the

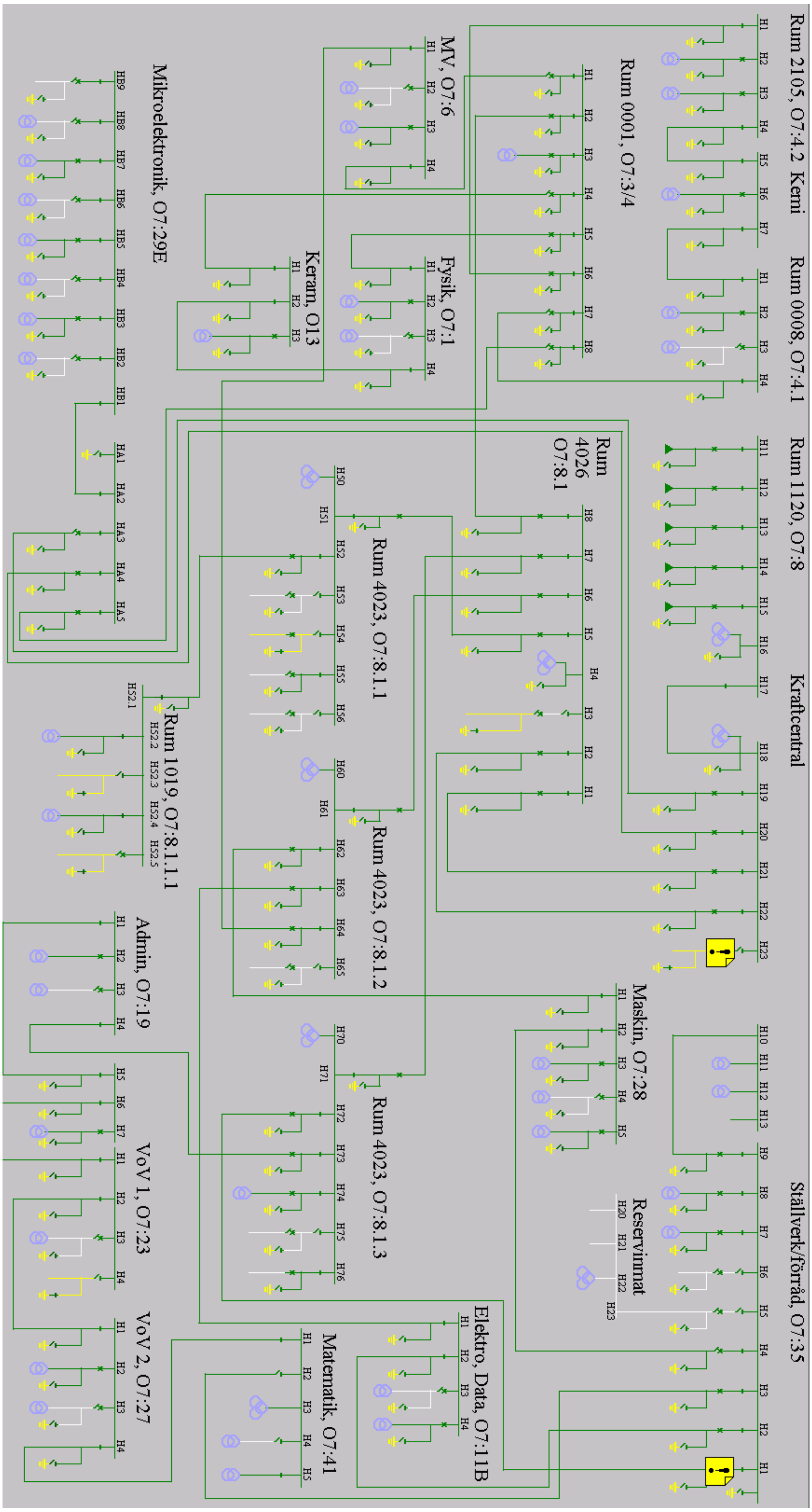

Figure 3.3: Overview of Chalmers grid within the Microscada system.

model can be refined.

$$CF = \frac{V_{measured}(h)}{V_{estimated}(h)} \tag{3.3}$$

where $V_{measured}$ is the mean value of the measured line-to-line voltages and $V_{estimated}$ is the assumed constant voltage of 400V line-to-line.

The results of the measurements are presented, where the voltages, currents and active power have been measured during half a day, with 1-hour resolution. Figure 3.4 shows the estimated and measured load profiles. It is visible that the two profiles are similar although some differences are seen. These might be due to measurements points being hourly, meaning that the instantaneous values of power differ from the mean power over the actual hour. The voltages shown in Figure 3.5 are experiencing small variations between 404 and 394 voltage, where the voltage is decreasing during high demand hours.

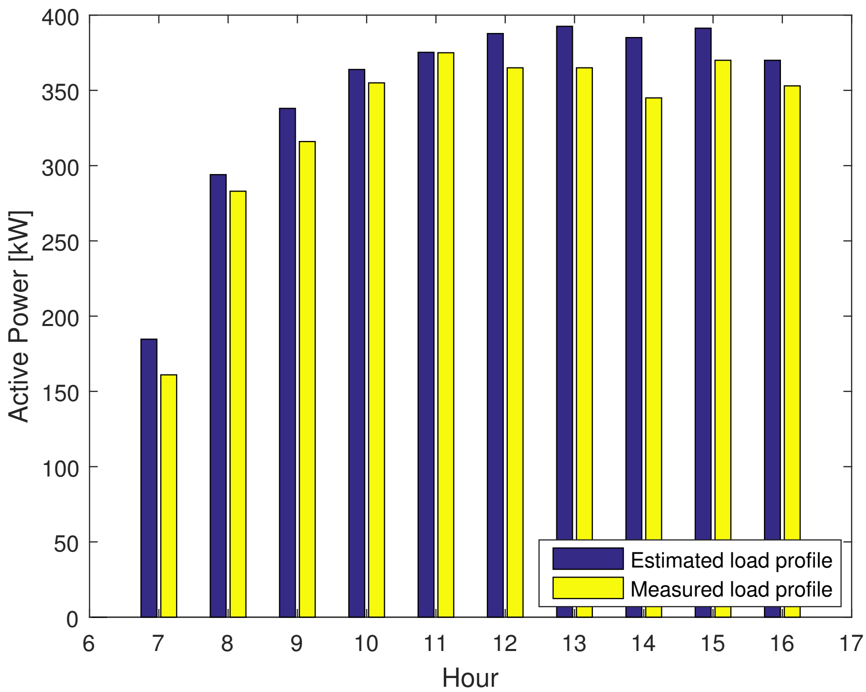

Figure 3.4: Estimated and measured load profile at bus 07:11B 13/5-2016

The NRMSE was calculated to 6.83%, and with the correction factor CF accounting for the voltage difference this error was reduced to 6.71%. This suggests that the cause of the error is not the assumption of 1 p.u voltage level. The fact that measurements were conducted taking one value per hour might affect the results since variations during each hour are not taken into account, thus it could be a possible cause of the error. Errors in current monitoring by Microscada could also be affecting the result.

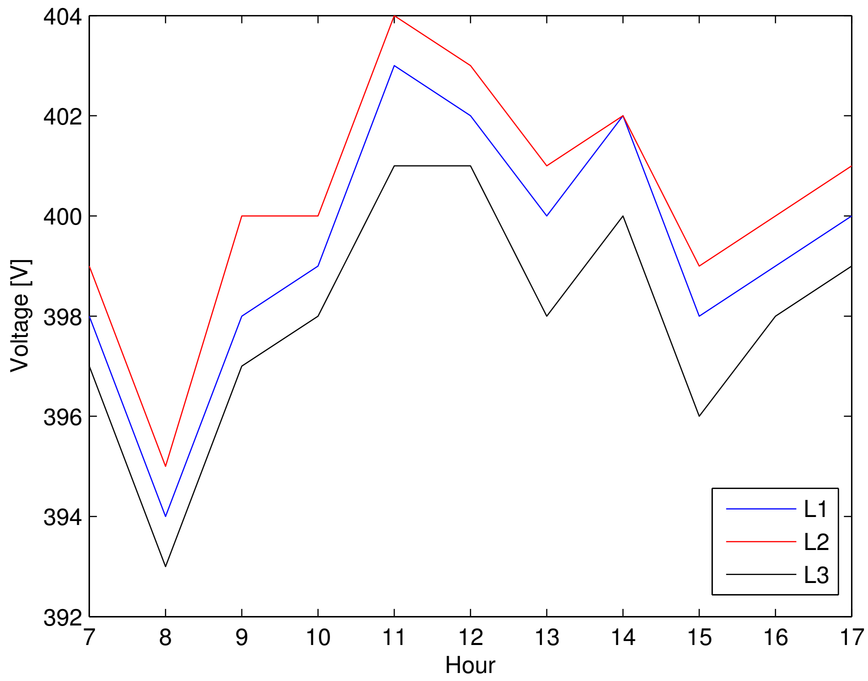

Figure 3.5: Measured voltages 13/5-2016

3.1.3 Grid data

The data required to create models of the network are acquired from Akademiska Hus. The data consists of cable dimensions, lengths, types of cables and transformer data such as ratings and impedance values. These data are necessary to construct an accurate model of the grid which is necessary in the optimal power flow calculations. The branch data for the network is shown in Table 3.1 and the transformer data are shown in Table 3.2. Note that the transformers do not have any resistance and are thereby assumed to be lossless. The bus numbers are according to the model developed in PSS/E which can be seen in Figure 3.6.

3.1.4 Generation data

There are currently three types of generation available in Chalmers' grid. These are power from the main grid and local generation with the CHP plant or the solar PV.

From grid

When operated under normal conditions Chalmers' grid receives power from the main grid operated by Göteborg Energi. This connection is seen as an endless power supply from the microgrid and can be bought using Nordpool day-ahead spot market prices [30].

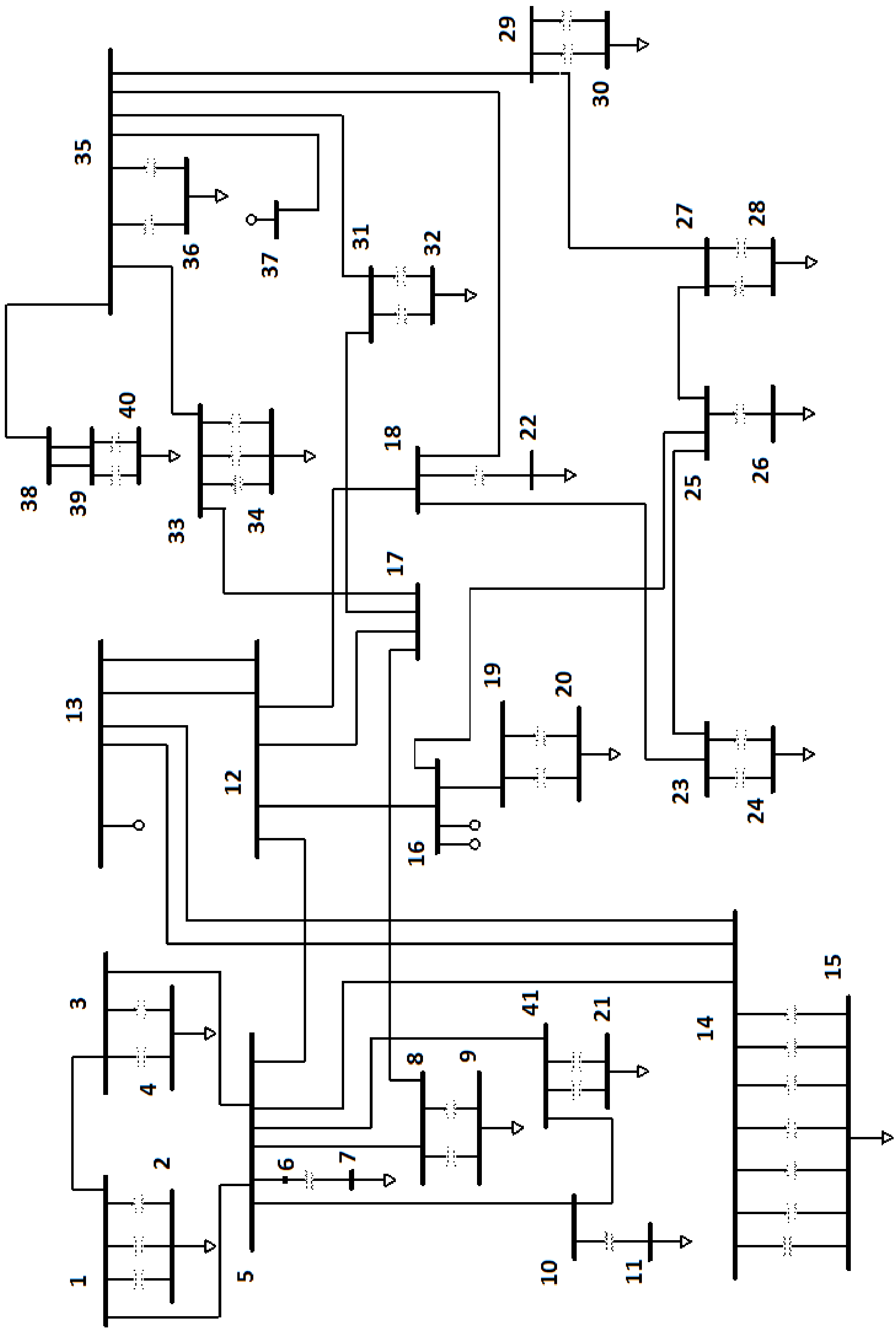

Figure 3.6: PSS/E single line diagram with bus numbers used within the PSS/E and GAMS models.

Table 3.1: Branch Data

From bus - To bus	Line-length [m]	R [$m\Omega$]	X [$m\Omega$]	Line-charging [μF]	Current-limits [A]
1-3	75	9.4	6.4	0.030	385
1-5	70	8.8	5.9	0.028	385
5-6	40	7.0	3.4	0.014	300
5-12	275	34.4	23.3	0.11	385
5-41	250	14.4	6.4	0.0245	385
8-17	110	13.8	9.3	0.0440	385
10-41	100	20.6	9.3	0.035	300
12-13	25	1.6	1.1	0.005	770
12-16	15	1.9	1.3	0.006	385
12-17	20	2.5	1.7	0.008	385
12-18	25	3.1	2.1	0.010	385
13-14	420	52.5	35.6	0.168	385
16-19	25	3.1	2.1	0.010	385
17-31	330	41.3	28.0	0.132	385
17-33	80	10.0	6.8	0.032	385
18-23	225	28.1	19.1	0.090	385
18-35	400	50.0	33.9	0.16	385
23-25	300	37.5	25.4	0.12	385
25-27	165	20.6	14	0.066	385
29-35	400	51.3	34.8	0.164	385
35-38	10	1.3	0.9	0.004	385
38-39	25	4.0	1.2	0.004	205

CHP plant

The CHP plant at Chalmers has a maximum electrical output power of 1 MW. To produce this amount of power there will also be heat generated, which has to be either used or sold. The cost of generation of the CHP plant, GC_{CHP}, is estimated to 600 SEK/MWh according to Akademiska Hus, not taking into account the benefits of possibly selling the produced heat.

Solar PV

A solar PV panel with a rated power of 15.7 kW is installed at a wall at Chalmers which is a part of the local generation and is assumed to have no cost associated with it. Two different methods have been used to get the power output from this solar PV depending on the time span the simulation is run for.

Short-term solar estimation

When the simulations are run for the short-term, 24 hours are considered. The output power profile seen in figure 3.7 is then used for estimate the solar power output and is a normalized output profile for three days during spring 2016, 22th

Table 3.2: Transformer Data

From-To	X [%]	Rating [kVA]
1-2	4.8	800
1-2	5.0	800
1-2	5.2	800
3-4	5.69	800
6-7	5.8	1000
8-9	5.8	800
10-11	4.82	800
14-15	5.0	1250
14-15	5.0	1250
14-15	4.9	1250
18-22	5.5	1250
19-20	6.31	800
19-20	5.0	800
21-41	5.7	800
21-41	6.3	1000
23-24	4.27	400
25-26	4.8	800
27-28	4.9	800
29-30	5.8	800
31-32	4.5	1250
33-34	6.3	800
33-34	6.3	800
35-36	5.2	800
35-36	4.9	600
39-40	5.2	1250
39-40	5.2	1250

of february, 30th of april and 12th of may. The data for these days is based on a 5.5 kW rated solar farm located in Gothenburg. It can be seen that the day in April is poor in solar irradiation while the day in February is a sunny day, thus the big difference between the two. The power output is calculated using equation 3.4 where P_{pv} is the output power from the solar cells, P_{solar} is the power output for hour h from figure 3.7. $P_{solar,rated}$ is the rated power of the solar panels.

$$P_{pv}(h) = P_{solar}(h) \cdot P_{solar,rated} \tag{3.4}$$

Medium-term solar estimation

Due to limitations in the data available from the solar panels used for the short-term model, the total beam irradiance is instead used to estimate the output power of the solar panels when the medium-term model is ran. The irradiance data is taken from System Advisor Model (SAM), which is a model software which also consists

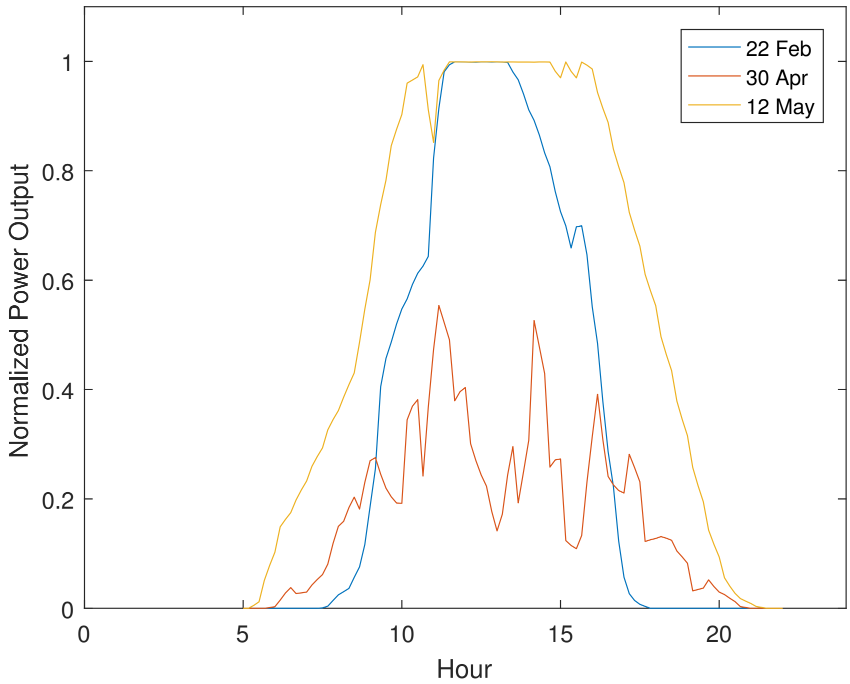

Figure 3.7: Normalized solar output profile

of a database with for example irradiance data. An irradiance profile for an average day for each month of the year is used to estimate the power output of the solar panels, giving a model which accounts for the changes in irradiation over the year. The irradiance data is presented in figure 3.8, where the Direct Normal Irradiance (DNI) for four months of the year is shown.
The power output of the solar cells is estimated using equation 3.5 where DNI_{STC} is the irradiance used for standard test conditions to calculate the rated power of solar cells, which is 1000 W/m^2 according to IEC 60904-3 [31]. $DNI(h)$ denotes the irradiance for each hour as shown in figure 3.8 and P_{rated} is the rated power of the installed solar cells.

$$P_{pv}(h) = \frac{DNI(h)}{DNI_{STC}} \cdot P_{rated} \tag{3.5}$$

3.1.5 Load profiles

Two different load profiles have been developed, one for the short-term model and an extended load profile for the medium-term model.

Short-term model

The simulations have been carried out based on a load profile for Thursday 17th of march 2016. This profile can be seen in table figure 3.9. It can be observed that there is a higher demand during the workday and the peak of 5472.9 kW occurs at hour 14. The total energy demand for 24 hours is calculated to be 105.5 MWh.

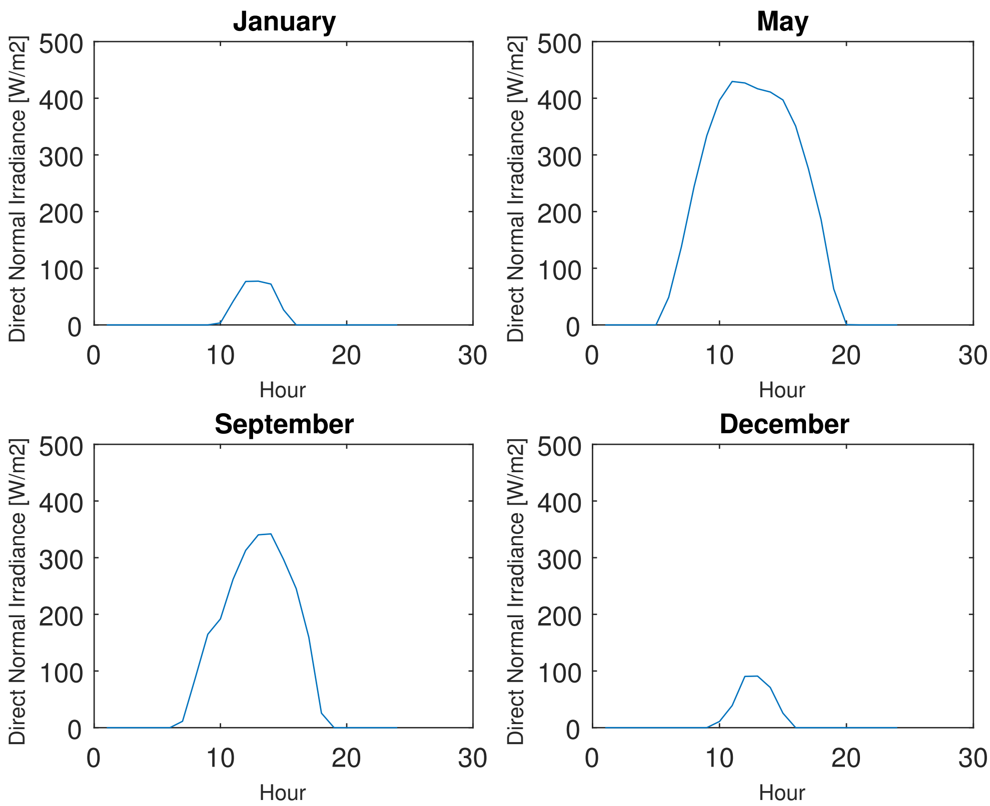

Figure 3.8: Irradiance data for Landvetter Göteborg

Medium-term model

To extend the load profile to be valid for the medium-term model, which has a time span of one year, the load profile presented for the one-day model was scaled with a factor based on the energy consumption variations over the year. This scaling factor is calculated by comparing the energy consumption for all buildings with the ones during the day which the short-term load profile was extracted. The scaling factor SF is then expressed as in equation 3.6.

$$SF(h) = \frac{E(h,d)}{E(h,76)} \tag{3.6}$$

where day 76 denotes the example day used for the one-day model.

The load is then estimated according to equation 3.7.

$$P_{load}(i,h,d) = P_{load}(i,h,76) \cdot SF(h) \tag{3.7}$$

This load scaling factor is presented in figure 3.10. It is shown that the load is reduced during the summer when the activity at campus is naturally lower. The variations between days is due to weekends having a lower energy consumption since there is no education being held at weekends.

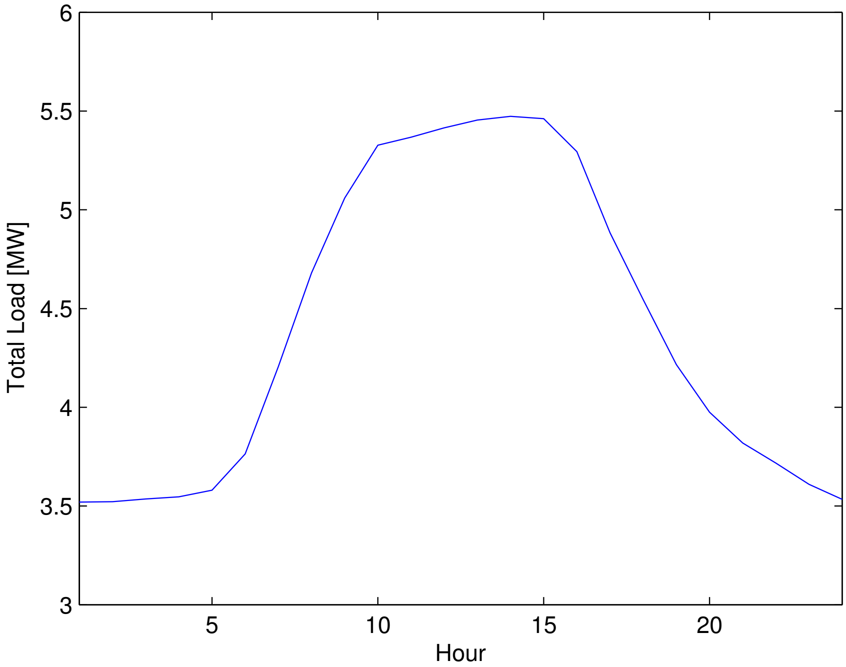

Figure 3.9: Load profile

3.2 Modeling

The modeling consists of three models, one load flow model in PSS/E and two OPF-based microgrid energy management models, one to simulate for one day and an extended model for one year simulations. The models consist of an optimization model in GAMS [32] and data management in MATLAB.

3.2.1 Power flow in PSS/E

A model of the network was constructed using Power System Simulator for Engineering (PSS/E) to visualize the network. The model includes grid data such as line impedance, transformer data and voltage levels. The PSS/E model is used to run a power flow with fixed values for loads to establish a base case for how the grid works. The model can later be used to validate the results from the EMM.
The one-line diagram of the PSS/E model is shown in Figure 3.6. It can be noted that the PSS/E model has 41 buses which is more than the single line diagram provided by Akademiska Hus. This is because extra buses are used to connect the load to the low voltage side of the transformers. Bus 13 is considered the slack bus of the system since this is the PCC where the main grid is connected to the microgrid.

3.2.2 OPF-based EMM for microgrids

The EMM model is constructed in GAMS to schedule generation and storage in the most efficient way based on the objective function which in this case is the total

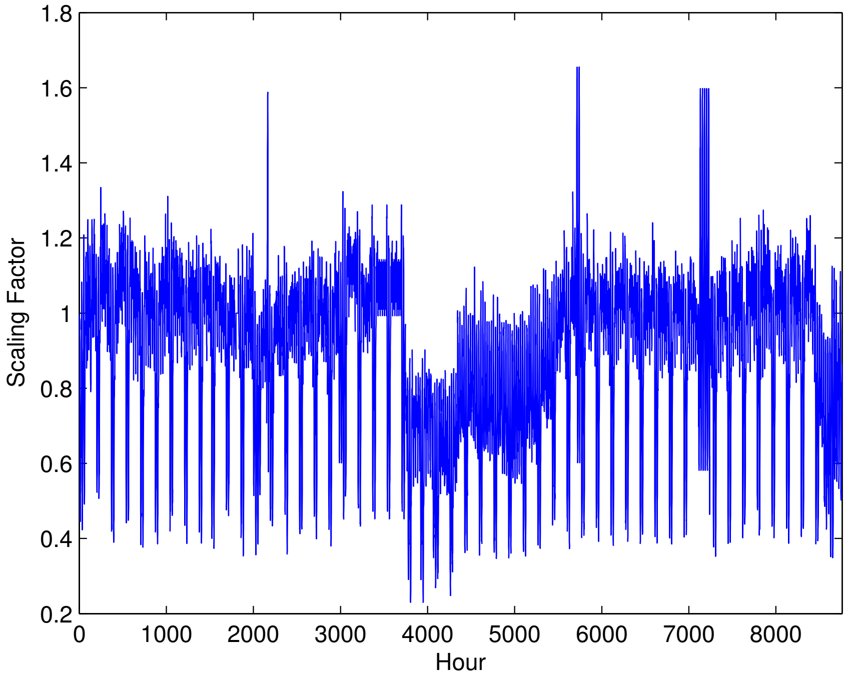

Figure 3.10: Load scaling factor for the extended microgrid model.

cost of electricity for campus Johanneberg at Chalmers. The objective function is minimized with respect to several constraints due to the characteristics of the grid. The constraints consist of power flow equations, transmission constraints, generation and load constraints and finally constraints regarding energy storage such as SOC constraints. Since some of the constraints are nonlinear the MINOS NLP (nonlinear programming) solver is used.

Objective Function

The objective function is expressed as seen in equation 3.8.

$$Cost = \sum_{h=1}^{n} \sum_{i=1}^{k} P_{CHP}(i,h)GC_{CHP}(i) + P_{grid}(i,h)Elprice(h) + PF\Delta P_{load}(i,h) \quad (3.8)$$

where $Elprice$ denotes the price from Nordpool day-ahead market for the grid power not including taxes. Taxes and other grid costs where not accounted for due to unavailability of data. P_{CHP} and GC_{CHP} denotes the generation and its cost of the local CHP generation. P_{grid} denotes the power injected by the main grid and PF denotes the penalty factor associated with load curtailment. The penalty factor is a fictive cost which is added in the objective function to control the load curtailment. This penalty factor determines when the flexible load should be activated so it is only used the most beneficial hours. It is assumed to be 240 SEK/MWh, meaning that the load curtailment will be activated only when the electricity price exceeds the mean electricity price with 20%. ΔP_{load} describes the down regulation possibilities at Chalmers which is estimated to 20% of the total ventilation power P_{fan}. The total power of the fans is 500 kW and is assumed to be distributed according to load levels. It is described by equation 3.13.

Power flow equations

$$\begin{aligned} P_{CHP}(i,h) + P_{grid}(i,h) - [P_{load}(i,h) - P_{pv}(i,h)] + P_{flex}(i,h) = \\ = \sum_{j=1}^{k} |V_i||V_j|(G_{i,j}\cos\theta_{i,j} + B_{i,j}\sin\theta_{i,j}) \end{aligned} \tag{3.9}$$

$$\begin{aligned} Q_{CHP}(i,h) + Q_{grid}(i,h) - Q_{load}(i,h) + Q_{flex}(i,h) = \\ = \sum_{j=1}^{k} |V_i||V_j|(G_{i,j}\cos\theta_{i,j} - B_{i,j}\sin\theta_{i,j}) \end{aligned} \tag{3.10}$$

where G and B are the real and imaginary parts of the admittance between bus i and j respectively, θ is the voltage angle difference between bus i and j, V_i and V_j are the voltages at bus i and j respectively. P_{load} is the static load for each hour h and bus i. [P_{load}-P_{pv}] denotes the residual load which is the total load P_{load} minus the generated power from solar PV P_{pv}. P_{flex} is the flexible load which consists of the battery storage power $P_{battery}$ and regulating power ΔP_{load}.

Flexible load constraints

P_{flex} and Q_{flex}can be expressed as seen in equation 3.11 and 3.12.

$$P_{flex}(i,h) = \eta_{dis} \cdot P_{dis}(i,h) + P_{chr}(i,h) + \Delta P_{load}(i,h) \tag{3.11}$$

$$Q_{flex}(i,h) = Q_{battery}(i,h) + \Delta Q_{load}(i,h) \tag{3.12}$$

where P_{dis} and P_{chr} is the power drawn or injected to the grid depending on charging or discharging of batteries and η_{dis} is the discharging efficiency.

Down-regulating constraints

$$0 \leq \Delta P_{load}(i,h) \leq 0.2 P_{fan}(i,h) \tag{3.13}$$

A change in active power ΔP_{load} also results in a change in reactive power ΔQ_{load} as described by equation 3.14

$$\Delta Q_{load}(i,h) = \Delta P_{load}(i,h) \cdot \tan\phi_{load}(i,h) \tag{3.14}$$

where $\phi_{load}(i,h)$ denotes the power factor. The power factor $\cos\phi_{load}(i,h) = 0.98$ lagging, according to measurements from substation 07:11B which gives the power factor ϕ_{load}. Since the power factor is difficult to measure at all buses at the same time is assumed to be constant for all buildings at Chalmers for every hour.

Generation and voltage constraints

The generation constraints sets the limit for the grid power and the CHP plant operation. During normal conditions there are no constraints on the grid power as can be seen in Equation 3.15 and 3.16.

$$P_{grid}(i,h) \leq \infty \tag{3.15}$$

$$Q_{grid}(i,h) \leq \infty \tag{3.16}$$

The limitation on the CHP generation is given by

$$0 \leq P_{CHP}(i,h) \leq P_{CHP}^{max} \tag{3.17}$$

$$-0.3 \cdot P_{CHP}^{max} \leq Q_{CHP}(i,h) \leq 0.3 \cdot P_{CHP}^{max} \tag{3.18}$$

where P_{CHP}^{max} is 1 MW.
The battery can act as both generation and load and the power output is limited by the maximum power output of the batteries. This is seen in Equation 3.19, 3.20 and 3.21.

$$P_{chr}(i,h) \leq P_{chr,max}(h) \tag{3.19}$$

$$P_{dis}(i,h) \leq P_{dis,max}(h) \tag{3.20}$$

$$-0.3 \cdot P_{battery,max}(h) \leq Q_{battery}(i,h) \leq 0.3 \cdot P_{battery,max}(h) \tag{3.21}$$

There are also constraints on the voltage levels within the grid which is seen in Equation 3.22.

$$V_{min}(i) \leq V(i) \leq V_{max}(i) \tag{3.22}$$

where $V_{min}(i)$ is 0.95 and $V_{max}(i)$ is 1.05.

Power flow constraints

The apparent power limitations are implemented as a current limitation which is provided by the cable manufacturer. The power limitation is described by equation 3.23.

$$-I_{lim}(i,j) \leq I(i,j) \leq I_{lim}(i,j) \tag{3.23}$$

3.2.3 Stationary battery energy storage system

The ESS in the grid enables demand response as well as functioning as a backup generation in case of a disconnection from the main grid. The microgrid is assumed to be able to function for one hour in island mode, thus the minimum size of the

ESS, $E_{battery,min}$, is equal to the highest load minus local generation during the day. The ESS is modeled as a load which can be either positive or negative which means it can be seen as both a source of generation and a load. To keep track of how much energy is currently stored within the batteries the SOC must be monitored. The state of charge is expressed as seen in equation 3.24.

$$SOC(i,h) = \frac{E(i,h)}{E_{rated}(i)} \tag{3.24}$$

where E is the total energy stored in the battery and E_{rated} is the total installed battery capacity.
The state of charge is limited between 0 and 1 as seen in equation 3.25.

$$0 \leq SOC(i,h) \leq 1 \tag{3.25}$$

The change in state of charge is expressed as

$$SOC(i,h) = SOC(i,h-1) + \frac{\eta_{chr} \cdot P_{chr}(i,h-1)}{E_{rated}(i)} - \frac{P_{dis}(i,h-1)}{E_{rated}(i)} \tag{3.26}$$

where η_{chr} is the charging efficiency.
The benefits associated with the ESS can be described by the difference between the total cost of electricity with and without ESS, as seen in equation 3.27.

$$Benefit = \sum_{h=1}^{n} Cost_{w/o,ESS}(h) - \sum_{h=1}^{n} Cost_{w,ESS}(h) \tag{3.27}$$

3.2.4 Electric vehicles

When electric vehicles is utilized as an ESS instead of a stationary ESS several new constraints is implemented, mainly to limit the SOC levels. The charging principle is the same as described in Equation 3.26 but since the vehicles must always be ready for usage the state of charge is limited to be at least 70 % during the entire day which is described by Equation 3.28

$$0.7 \leq SOC(i,h) \leq 1 \tag{3.28}$$

It is also assumed that the vehicles arrive at 08:00 and leave at 17:00 and has a SOC of 80 % at both these times, which is described by Equations 3.29 and 3.30. The vehicles are connected to the grid at bus 12 according to figure 3.6.

$$SOC(i, 17 + m \cdot 24) = 0.8 \tag{3.29}$$

where m = 0,1,2...

$$SOC(i, 8 + m \cdot 24) = 0.8 \tag{3.30}$$

3.2.5 Island mode constraints

To be able operate the microgrid in island mode additional constraints on the ESS is required. The energy in the ESS must always be enough to supply the microgrid for the desired island mode operation time. The SOC limit is then updated with respect of this required limitation as can be seen in equation 3.31

$$\frac{6 \cdot t}{E_{rated}(i)} \leq SOC(i,h) \leq 1 \tag{3.31}$$

where t is the time of desired island mode operation in hours. For the worst case scenario, the ESS must supply 6 MWh to the grid for each hour the microgrid is operated in island mode.

3.2.6 Microgrid simulation platform

The Microgrid Simulation Platform (MSP) is built up with both GAMS and MATLAB where all input and output data can be viewed and processed within MATLAB. The MSP structure is shown in figure 3.11. The reason for using both programs is the possibility of changing input data and running numerous simulations with varying input in a simple way. The MSP consists of the MATLAB scripts, excel files containing input data and the EMM within GAMS. Other parameters such as storage location or size can also be altered from MATLAB.

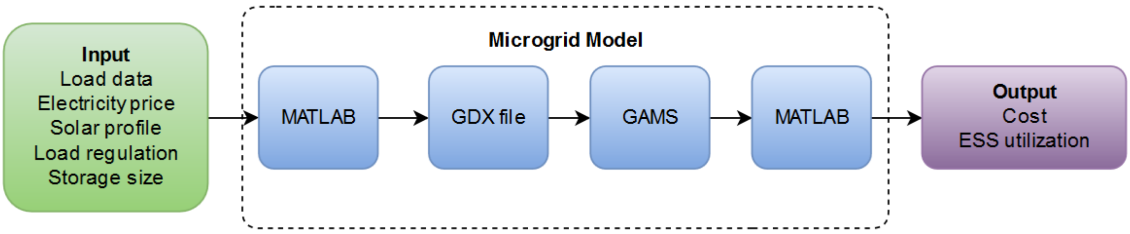

Figure 3.11: Flowchart of the microgrid simulation platform

3.3 Short-term model (24-hour)

When the EMM is run for a short-term time period, which is 24-hours, the suitable load profile and solar PV generation is used, as described in Section 3.1.5 and 3.1.4. The constraints used are Equation 3.8 to 3.27. The island mode simulations are also made using the short-term model and for those cases the Equation 3.31 replaces Equation 3.25.

3.4 Mid-term model (One year)

The medium-term model, , which use a time period of one year, is used to evaluate the optimal sizing of the ESS, as well as studying the behavior of the microgrid in a more detailed manner. This led to adjustments in load profile and solar PV power which is described in Section 3.1.5 and 3.1.4. The same equations as in the short-term model are used, however, due to simulation difficulties the line constraints, given by Equation 3.23, are excluded. Due to complexity of running simulations over the whole year at once, the model was designed to run the EMM for each month individually, thus running 12 separate simulations after each other to simulate an entire year.

3.5 Validation of load flow model

The PSS/E model is used to validate the accuracy of the GAMS model. A snapshot of the power flow for one hour from the PSS/E model is used to compare the bus voltages and angles in the grid to the values obtained from the GAMS model while running a power flow with the same load. The results are presented in figure 3.3. The results from the two simulations show that there is no difference in voltage levels for any bus and there are some slight difference for the voltage angle. The largest differences in angle occurs at bus 20 where the difference is -0.21 degrees. This is most probably due to differences in the matter of solving the power flow equations. This shows that the EMM solves the power flow as intended.

Table 3.3: Model validation, comparison of bus voltages and angles between PSSE model and GAMS model.

	PSS/E-model		**GAMS-model**			
Bus	**Voltage [pu]**	δ **[deg]**	**Voltage [pu]**	δ **[deg]**	ΔV **[pu]**	$\Delta\delta$ **[deg]**
1	0.999	-0.02	0.999	-0.01	0.00	-0.01
2	0.996	-1.00	0.996	-0.97	0.00	-0.03
3	0.999	-0.02	0.999	-0.01	0.00	-0.01
4	0.995	-1.14	0.995	-1.20	0.00	0.06
5	0.999	-0.01	0.999	-0.01	0.00	0.00
6	0.999	-0.01	0.999	-0.01	0.00	0.00
7	0.998	-0.42	0.998	-0.40	0.00	-0.02
8	0.999	0.00	1.000	0.00	0.00	0.00
9	0.996	-1.07	0.996	-1.09	0.00	0.02
10	0.999	-0.01	0.999	-0.01	0.00	0.00
11	0.999	-0.15	0.999	-0.17	0.00	0.02
12	1.000	0.00	1.000	0.00	0.00	0.00
13	1.000	0.00	1.000	0.00	0.00	0.00
14	0.999	-0.02	0.999	-0.02	0.00	0.00
15	0.996	-0.95	0.996	-0.97	0.00	0.02
16	1.000	0.00	1.000	0.00	0.00	0.00
17	1.000	0.00	1.000	0.00	0.00	0.00
18	1.000	0.00	1.000	0.00	0.00	0.00
19	1.000	0.00	1.000	0.00	0.00	0.00
20	0.998	-0.55	0.999	-0.34	0.00	-0.21
21	0.998	-0.44	0.998	-0.46	0.00	0.02
22	0.997	-0.78	0.997	-0.80	0.00	0.02
23	1.000	-0.01	1.000	0.00	0.00	-0.01
24	0.996	-0.23	0.999	-0.23	0.00	0.00
25	0.999	-0.01	1.000	-0.01	0.00	0.00
26	0.995	-0.90	0.996	-0.92	0.00	0.02
27	0.999	-0.01	0.999	-0.01	0.00	0.00
28	0.995	-1.13	0.995	-1.15	0.00	0.02
29	1.000	-0.01	1.000	0.00	0.00	-0.01
30	0.998	-0.61	0.998	-0.63	0.00	0.02
31	1.000	-0.01	1.000	0.00	0.00	-0.01
32	0.997	-0.74	0.997	-0.75	0.00	0.01
33	1.000	0.00	1.000	0.00	0.00	0.00
34	0.996	-1.14	0.996	-1.15	0.00	0.01
35	1.000	-0.01	1.000	0.00	0.00	-0.01
36	0.999	-0.34	0.999	-0.34	0.00	0.00
37	N/A	N/A	N/A	N/A	N/A	N/A
38	1.000	-0.01	1.000	0.00	0.00	-0.01
39	1.000	-0.01	1.000	0.00	0.00	-0.01
40	1.000	-0.03	1.000	-0.02	0.00	-0.01
41	0.999	-0.01	0.999	-0.01	0.00	0.00

4

Cost-benefit analysis for selection of battery energy storage options

This chapter treats the cost-benefit analysis used to establish the optimal location and size of the ESS. This analysis compares the annual energy cost based on a Capital Recovery Factor (CRF) for different configurations of the ESS. First the location is evaluated based on the short-term model with respect to both energy cost and losses. Then a cost-benefit analysis is made with different ESS sizes to evaluate the best size.

4.1 Investment cost evaluation

To evaluate the present value of an annuity, the CRF described in 4.1 can be used.

$$CRF = \frac{i(1+i)^n}{(1+i)^n - 1} \tag{4.1}$$

where i is the interest rate, and n denotes the depreciation period. Assuming a battery lifetime of 5 years and a interest rate of 5%, using equation 4.1, the CRF is calculated to 0.231. The ratio between the investment cost and benefits of the investment is a deciding factor regarding ESS. By multiplying the investment cost with the CRF the annuity of the investment can be calculated and compared to the annual revenue gained from the ESS. The annual investment cost, C_{ESS}, is calculated as shown in equation 4.2. The investment cost, C_E, is multiplied by the capital recovery factor to get the annual cost which can be compared to the annual benefits of the ESS.

$$C_{ESS} = CRF \cdot E_{Rated} \cdot C_E \tag{4.2}$$

Li-ion batteries are considered due to their high energy density compared to other batteries, which is beneficial in large scale storage systems [7]. The cost of Li-ion battery storage is estimated to $300 per kWh for the leading manufacturers of BEVs [10].

4.2 Optimal selection criterion

The sizing is composed of two parts, maximum power output and energy capacity.

The energy capacity and maximum power output was determined with regards to the total benefits due to storage in comparison to the investment cost. The ratio between benefits and investment cost is a deciding factor for the optimal size of the energy storage. This process is described by figure 4.1.

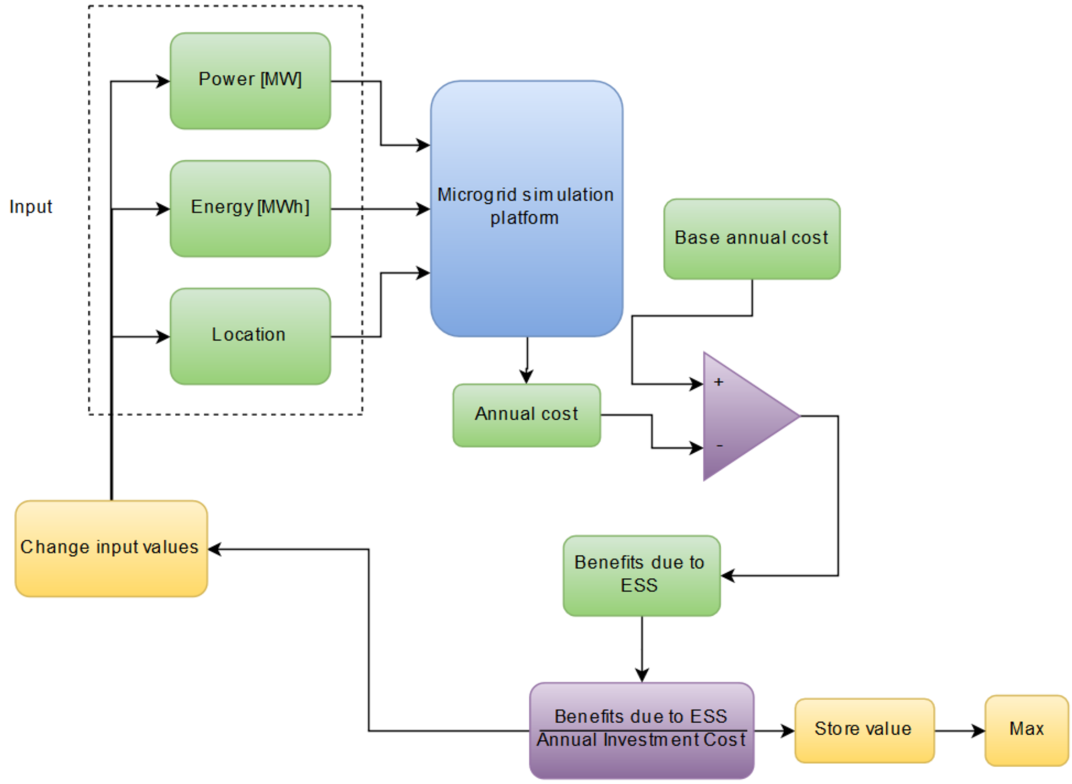

Figure 4.1: Flowchart of storage system design methodology

Location was determined by simulating an ESS at a few chosen locations of the grid, one of them being at the PCC, another at the midpoint of the grid, and finally at the highest loads in the grid. These cases were evaluated with respect to benefits gained from the ESS and the losses.
The energy storage can be either aggregated so that the storage is located in one spot, or spread out over numerous locations of the grid. The losses are of interest when choosing a location for the energy storage to obtain maximum benefits from the installed storage.
The optimal ESS is determined by the size and location which results in the highest ratio between total benefits and annual investment cost. Benefits is defined as the difference in operating cost of the MG with and without ESS, as described in equation 3.27.

4.3 Energy storage system sizing and location

This section displays the results of simulations regarding ESS sizing. Optimal location, maximum power output and energy capacity of the ESS are established.

4.3.1 Optimal location

To evaluate the optimal location of the ESS, losses and total benefits of the ESS was compared for 8 different cases containing both aggregated and distributed energy storage, however, the total ESS size is the same for all cases. These locations chosen to be evaluated was the PCC, the two highest loads, L1 and L2, and the bus 07:8.1. Due to the size of the model while using line constraints, it was not possible to simulate for the whole year. Instead the short-term model was used to simulate the different cases. The size of the ESS during these simulations was chosen to be 6 MWh and the results can be seen in table 4.1.
Having the ESS at the PCC was found to provide the lowest total cost of energy and losses while having it at L2 proved to be the worst location in both total energy cost and losses. There is little difference between having the ESS as a distributed storage and having it installed as a central ESS at the PCC. This is due to the low losses within the system, which is reasonable considering the cables in the grid are over dimensioned. With an increase in battery size the current limits of the cables might be exceeded during charging and discharging of the ESS for certain locations leading to a higher cost since the ESS cannot be operated optimally. At the PCC this issue will never occur which further implies the optimal location of ESS is at the PCC.

Table 4.1: Total cost for one day with different ESS locations

Storage Location	Benefit [SEK]	Loss [kW]
PCC	1078.50	40
PCC,07:8.1	1078.40	41
L1,L2,PCC,07:8.1	1078.20	43
07:8.1	1078.00	43
L1,PCC	1077.40	46
L2,PCC	1077.30	48
L1	1072.30	69
L2	1071.10	75

4.3.2 Optimal size

The total benefits is determined using the EMM, simulating a year of operation. Benefits due to energy storage for different battery capacities is shown in figure 4.2 and it is shown that they are increasing with an increased ESS capacity, however with a decreasing rate.
The benefits to investment cost ratio is shown in figure 4.3. For the investment to be economically beneficial the ratio would need exceed to 1. However, as can be seen, the ratio is much lower than 1 meaning that the investment is, from a pure economical point of view, not beneficial. There is a decreasing trend in ratio as the ESS size increases which means that an increase in installed ESS capacity increases the investment cost more than the benefits are increased. The variations seen in the figure could be due to simulation issues, at some months the GAMS-model was

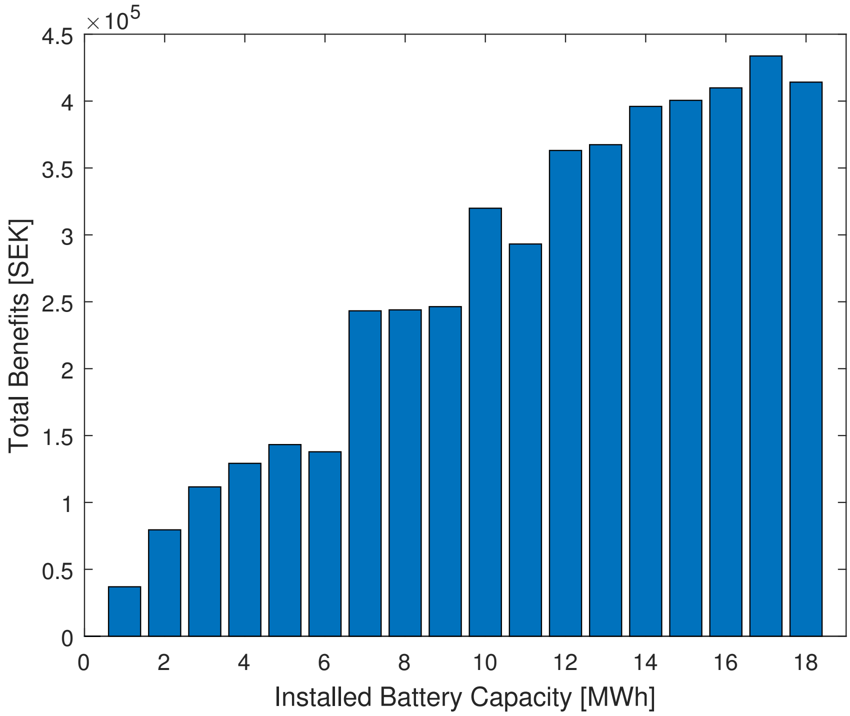

Figure 4.2: Benefits of battery storage for one year, displayed for different ESS sizes

not able to find an optimal solution due to a high number of non-linearities in the model formulation. However, the trend is clear despite these variations. This means that the optimal ESS size will depend on the island mode operation that is desirable since simulations do not show a profitable benefit to cost ratio. Instead the optimal size comes down to what cost the grid operator is willing to pay for the increased reliability of enabling island mode operation.

4.3.2.1 Sensitivity analysis

A sensitivity analysis is based on changing the parameters used to calculate the CRF for the investment. With varying lifetime and interest rate the benefit to investment cost ratio is calculated and shown in figure 4.4. It is shown that with a lower interest rate as well as a longer lifetime of batteries, the investment is considerably better. With dropping prices of energy storage the benefit to cost ratio could be further increased.
Figure 4.5 shows the benefit to cost ratio with different prices of batteries, in $\$/MWh$. The lifetime is assumed to 10 years and an interest rate of 3% is used in this case. It is also shown from figure 4.5 that the benefit to cost ratio is nonlinear for different prices since the ratio between \$200 and \$100 is larger than that between \$300 and \$200. This implies that the lower the prices get the better the investment, thus it could have future economical potential to include ESS in the grid.

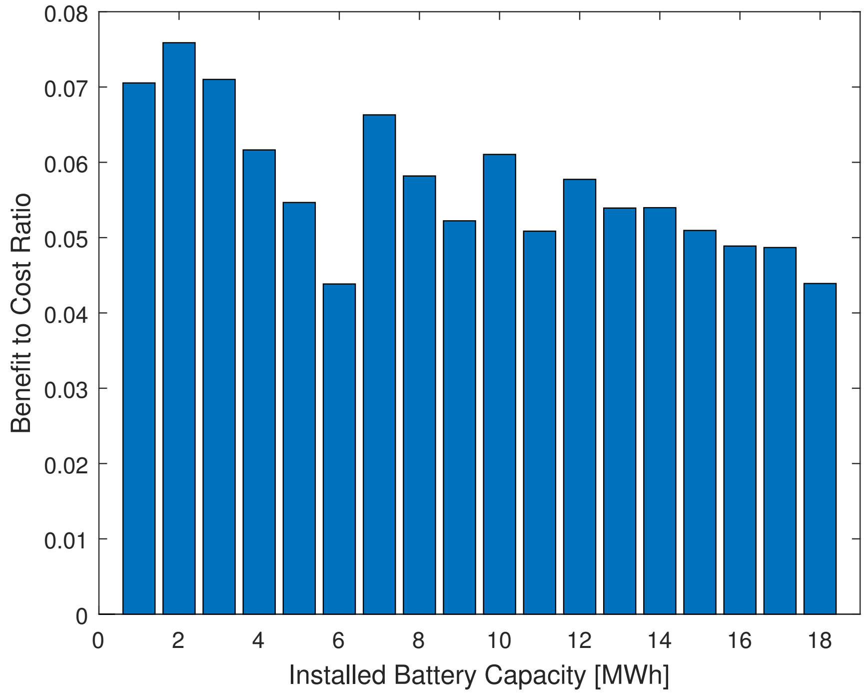

Figure 4.3: Benefit to investment cost ratio for different amount of installed storage.

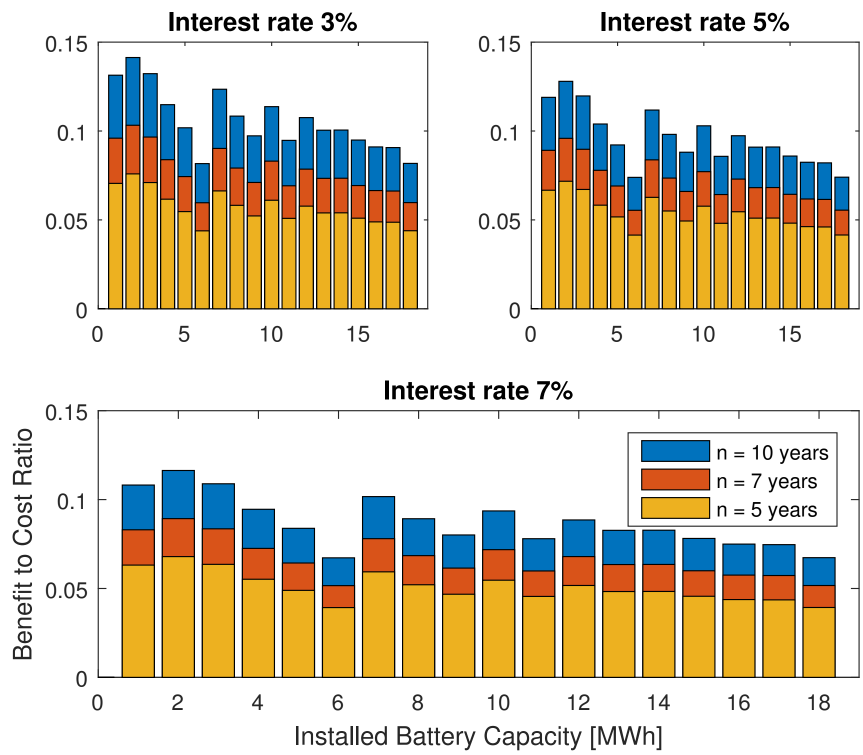

Figure 4.4: Benefit to investment cost ratio for different interest rates and expected lifetimes of storage.

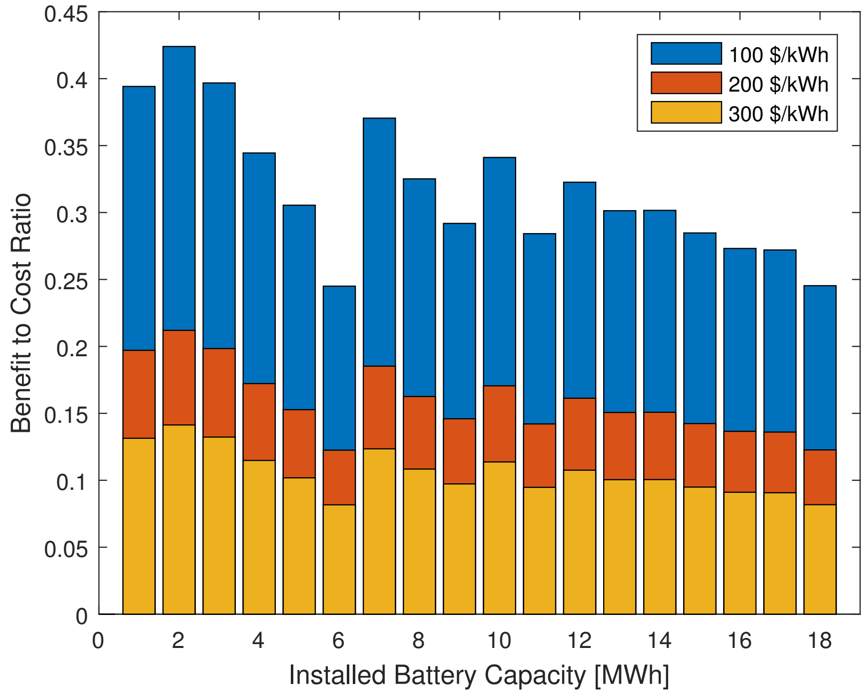

Figure 4.5: Benefit to investment cost ratio for different battery prices.

5

Evaluation of Chalmers microgrid operation scenarios

In this chapter the different cases are described and evaluated. There are four cases simulated, the first one is the base case when the grid is operated with and without any storage. The second is island mode to illustrate how the batteries operate during a disconnection from the main grid. The third one is when an increased renewable energy generation is present and finally the fourth case is when there is an EV fleet available to act as an ESS.

5.1 Case study

The case studies uses the MSP to evaluate how the system will behave and what benefits there are by operating the grid as a microgrid during certain circumstances.

5.1.1 Grid connected mode (Base case)

The grid is simulated using the EMM both with and without an ESS and the gained benefits are then evaluated. An evaluation of the benefits for running Chalmers' gird as a microgrid in its current state and with an ESS is then made.

5.1.2 Island mode

If there is an outage in the main grid the microgrid can be switched to island mode. To evaluate this, two 1-hour outages where simulated and the grid behavior was observed. The ESS together with the local generation is then expected to keep the microgrid running for the duration of these outages.

5.1.3 Increased renewable generation

With an increased amount of renewable generation the benefit of having a microgrid is expected to be higher. In order to verify this, different levels of generation from solar PV was simulated to compare the benefits gained with the base case. The amount of solar PV generation is currently 15.7 kW. Besides from this value, a range from 0 to 3MW are simulated.

5.1.4 Vehicle to grid

If there was a significant electric vehicle fleet located at Chalmers, their batteries could be used as distributed ESS within the microgrid. However, this type of ESS is mobile and might not be available when desired. The vehicles also need to be available for driving during all hours of the day so only a portion of their energy can be used within the microgrid. Assumptions for these simulations are as following:

- Number of vehicles simulated where 25-300, each with a 90 kWh battery installed [33]. Theses vehicles provide a total of 27 MWh of energy when all vehicles are connected.
- The vehicles are available within the grid between hour 8 and 17.
- The SOC equations are updated in order to ensure that the vehicles can be utilized during the day. The new equations specify that the batteries can be varied between 70 and 100% of their full capacity and they need to be at 80% charge at hour 17 which is seen in equation 3.28 and 3.29. The average charge is assumed to be 80% when the vehicles arrive in the morning which is described by equation 3.30.
- The net charge gain is assumed to be 0 which means that the vehicles leave with the same charge as they have when they arrive. It is modeled like this to simulate the benefits of energy exchange between the vehicles and the grid, not including the cost of charging vehicles to full.

5.2 Case study results

This section handles the case studies conducted in the project. The results of the case studies are presented and discussed.

5.2.1 Grid connected mode (Base case)

The results for different cases where the grid is operated in grid connected mode is presented in this section. The cases investigated are when no management is done and when the EMM is implemented, both with and without storage.

- The total annual energy cost for the case where no energy management is done is 7.0119 MSEK.
- When load curtailment is utilized the total annual energy cost is 7.0062 MSEK, a reduction of 5700 SEK/year.
- For the case when both load curtailment and a 2 MWh ESS is utilized the total annual energy cost is 6.9324 MSEK, a reduction of 79500 SEK/year.

The benefits when simulating the microgrid without any storage is small compared to the total energy cost and thus a poor incentive to implement it. However, the only load reduction taken into consideration is the ventilation power which could be reduced by 20 %, resulting in a total of 100 kW load reduction. If more flexible loads could be identified the total benefits would be expected to increase. Another factor which affects the benefits is the penalty factor which decides when the load curtailment is activated. This factor was set to 240 SEK/MWh, which is 20 %

higher than the mean electricity price for 2015. By lowering this factor the annual benefits would increase by operating the load curtailment more frequently.
Power bought from the grid for the cases without EMM and with EMM where a 2 MWh ESS is installed for 24-hours (based on data from 17/3-2016) can be seen in Figure 5.1. It can be noted that the ESS has two charging patterns during the day, one in the morning and one in the afternoon, and load curtailment is activated at hour 10.

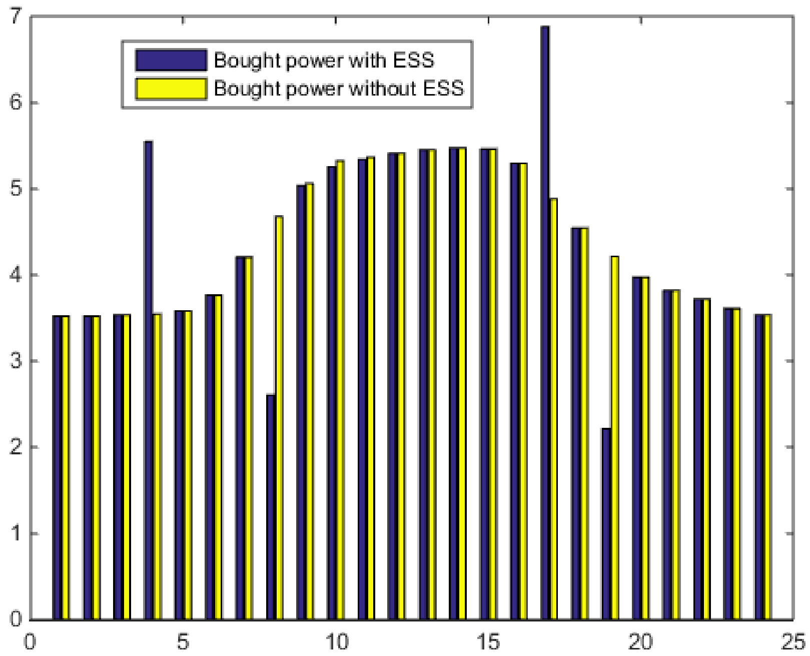

Figure 5.1: Power bought from the grid when EMM is used including ESS and without EMM.

5.2.2 Island mode

The minimum sizing of energy storage is determined by its ability to enable the microgrid to operate in island mode for a certain time. When the microgrid operates in island mode, the ESS must be able to supply enough power so that the the ESS together with local generation can supply the demand. Thereby the minimum power and energy capacity are determined by the maximum load and for how long the microgrid is to be operated in island mode. The minimum power and energy for the ESS are determined by equation 5.1 and 5.2.

$$P_{ESS,min} = P_{load,max} - P_{CHP} - 0.2P_{fan} \tag{5.1}$$

$$E_{ESS,min} = P_{ESS,min} \cdot h \tag{5.2}$$

where h denotes the amount of hours for which the microgrid is operated in island mode.

A fault at the PCC means that no power can be delivered to the microgrid from the main grid. This is simulated by setting the grid power to 0 for hour 4 and 17, thus forcing the ESS to supply the load together with local generation. Figure 5.2 shows the supply of power within the microgrid for 24 hours with the grid power outage explained. It can be seen that the ESS is operated to supply the loads when the grid power is set to zero. It can also be seen from the simulated fault in the afternoon that the CHP plant is operated in order to supply the loads, since the power from the battery is not enough to supply the entire load.

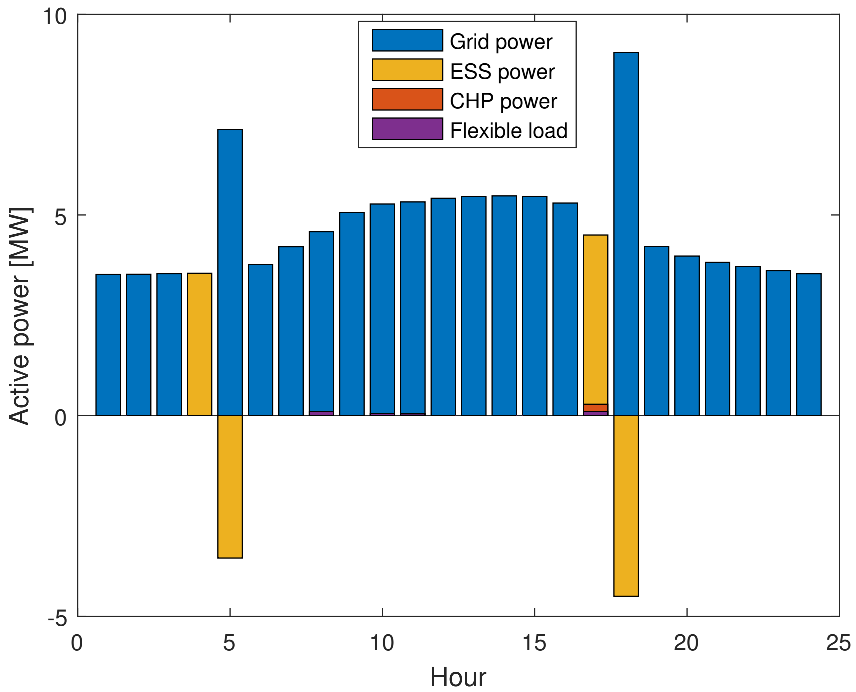

Figure 5.2: Island mode operation with two 1-hour outages

The total energy cost for 24-hours, both in normal conditions and with two 1-hour outages, can be seen in Table 5.1. It can be seen that the cost when island mode is utilized is 224 SEK higher than for normal operations. This cost increase will heavily depend on when the faults occur during the day since both the total load and the electricity price varies. In this case the disconnection was forced due to a fault but it might also be beneficial from an economical point of view to disconnect during certain hours if the ESS is large enough.

Table 5.1: Total energy cost for 24-hours for normal operation and with two 1-hour outages.

	Normal operation	Two 1-hour faults
Cost [SEK]	22400	22624

5.2.3 Renewable energy sources

An increase in the amount of renewable energy sources within the microgrid was investigated, where the solar PV output power was increased. Simulations using the EMM were conducted for values between 0 and 3 MWp from solar PV. The lifetime of solar cells used in the simulation is 20 years, and for the batteries 5 years. An interest rate of 5% is assumed and the cost associated with solar PV installation is 1€/Wp [34]. However, the price of solar power is not including any government grants, thus the total investment cost could be decreased further. As for other simulations the battery cost is 300$/MWh. The results are displayed in figure 5.3. It is shown that the maximum benefit to cost ratio is obtained with no ESS installed, but with increased solar power. It is also shown that for a fixed battery size, an increase in solar power also increases the benefits gained from ESS. Since the solar PV output power is depending on the radiation, the location is of great importance. In Sweden solar power is not as beneficial as in other countries with more sun hours during the year, which could explain why the benefits to cost ratio is not higher than what is shown in figure 5.3.

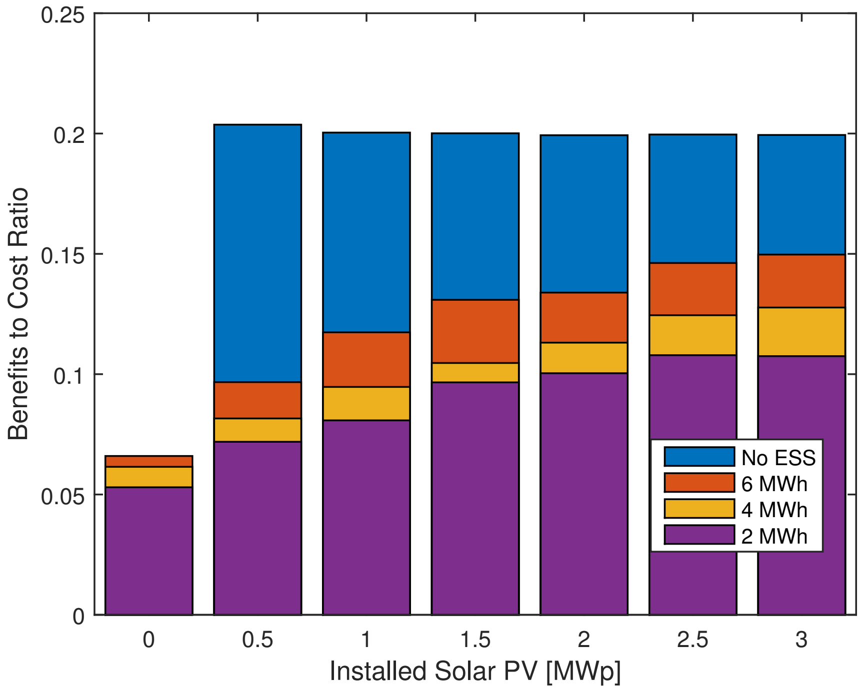

Figure 5.3: Benefits to investment cost ratio for different ESS sizes, with varying amount of installed solar power.

5.2.4 Vehicle to grid

The total cost for one year is shown in figure 5.4 assuming the EVs arrive at hour 8 and leave at hour 17. The cost is decreasing with an increased amount of EVs, which is essentially the same as increasing the ESS size. It can be seen that the benefits of

having 300 EVs is approximately 100 000 SEK annually, which corresponds to 330 SEK per car owner. Such a benefit is a quite poor incentive for car owners to take part in the V2G system since it will cause the lifetime of their batteries to decrease. The cost reduction is lower than what is accomplished by installing battery storage, and is likely because the EVs are not present during nighttime, therefore the benefits gained by charging batteries during the low price at night cannot be accomplished when using V2G.
The charging pattern is displayed in figure 5.5 where both SOC and power output from the EV fleet is shown. It can be seen that the EVs always have at least 70% charge left during the day so they can be operated if needed. The EVs are also charged up to 80 % before they leave so the resulting change of energy during one day is 0.

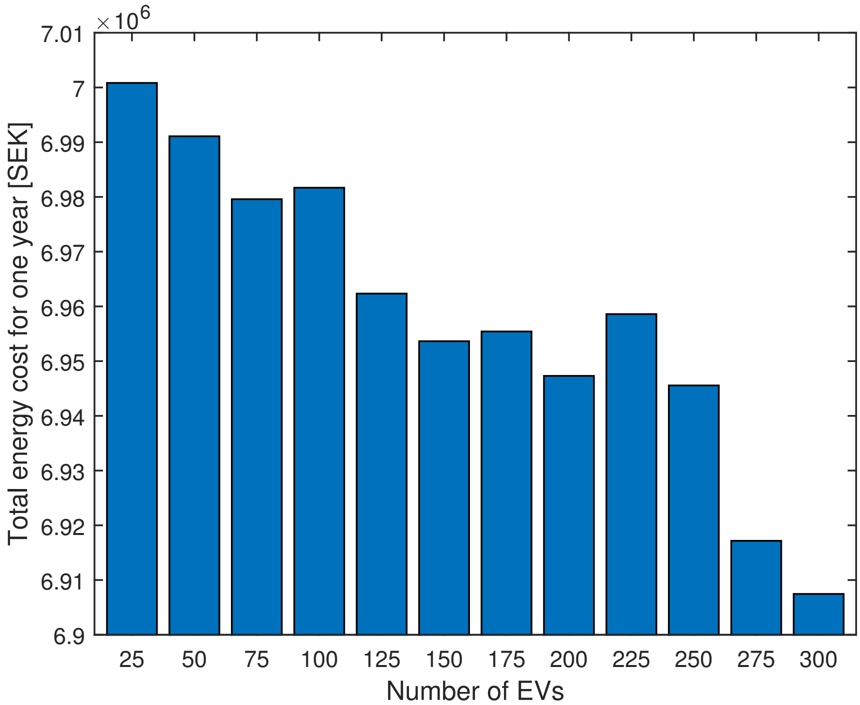

Figure 5.4: Total cost for one year vs number of EVs.

5.3 Reliability analysis

A microgrid should be able to operate independently from the main grid, and therefore increase its reliability. The amount of local generation and installed ESS will increase the ability to operate in island mode. Different levels of local generation and ESS sizes where evaluated based on the annual investment cost, annual benefits and their ability to operate in island mode. The results can be seen in table 5.2.
Since solar power is an unreliable resource it might not be available during disconnection from the main grid, hence the total time in island mode will therefore vary for the same installed solar capacity. It can be noted that the system can't be op-

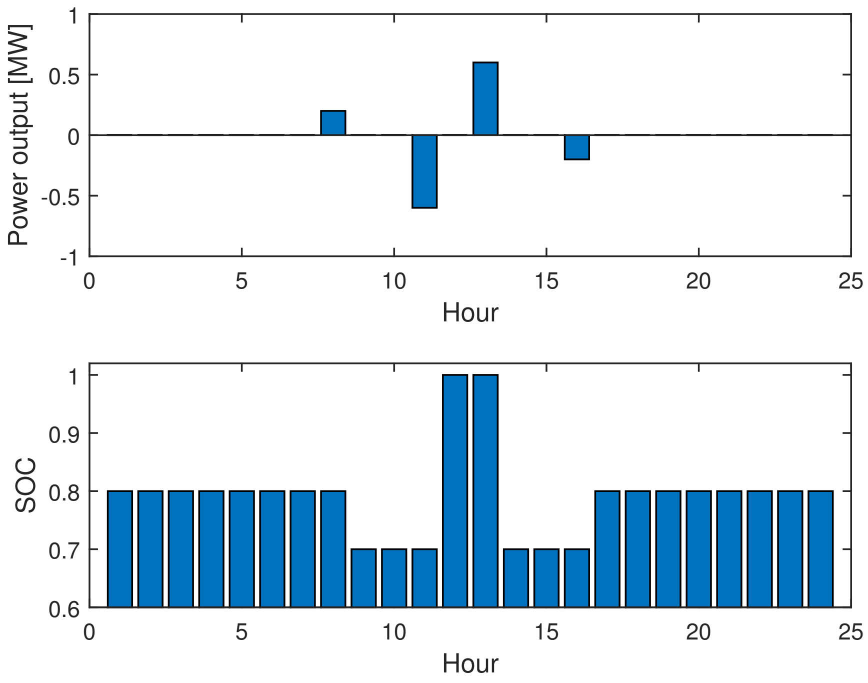

Figure 5.5: Output power P_{EV} and SOC during one day of operation.

erated in island mode without any ESS for the solar levels tested. This is due to the power levels the peak load requires to operate. There is a possibility to operate parts of the microgrid with only solar installed at these levels, however, this has not been investigated further.
The enhancement of reliability within the system comes from the battery storage, and can be associated with a cost which comes from the annual investment cost and the annual benefit. By subtracting the benefits from the annual investment cost, the total cost per hour of island mode can be calculated. For battery storage of 6 MWh this cost is calculated to 1.684 MSEK/year for one hour of island mode capability.

Table 5.2: Comparison of different investment costs, annual revenues and island mode operation times for different ESS and solar PV sizes

Installed battery capacity [MWh]	**Installed solar power [MWp]**	**Annual investment cost [MSEK]**	**Annual benefit [MSEK]**	**Island mode operation [h]**
0	0	0	0	0
0	3	2.17	0.432	0
2	1.5	1.70	0.287	0.33-0.5
2	3	2.79	0.490	0.33-0.66
4	1.5	2.33	0.345	0.66-0.8
4	3	3.41	0.560	0.66-1.0
6	0	1.86	0.176	1
6	3	4.03	0.590	1-1.33

The different sizes for the ESS investigated were 2, 4 and 6 MWh. Paired with 3 MWp solar PV installed, the island mode operation time can be seen in Figure 5.6.

There are two contributions to the total island mode time: first the reliable time which comes from batteries and secondly the unreliable time from solar PVs. These times are based on a worst case scenario meaning that the load is at its peak value. Other means of improving island mode operation time could be to increase reliable local generation, such as CHP. However, no investigation on this has been made.

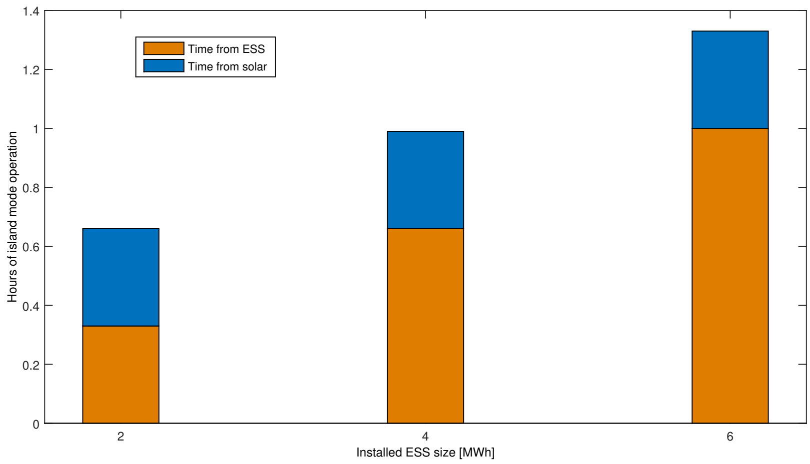

Figure 5.6: Island mode operation time for different ESS sizes with 3 MWp solar PV installed

The total energy cost can be reduced by introducing battery storage in the microgrid, or by investing in increasing the amount of solar PV. Figure 5.7 compares the total energy cost for one year. The base case is compared to different ESS sizes, with EVs and also for one case with 6 MWh of battery storage and 3 MWp of solar power. The total energy cost is reduced when more energy storage is installed, however the maximum cost reduction is obtained by including both battery storage and increasing the amount of solar PV. Including EVs as a mean of storage within the grid reduces the cost by 2.49%. The total energy cost can be reduced by as much as 8.43% when including both battery storage and increasing the amount of solar PV.

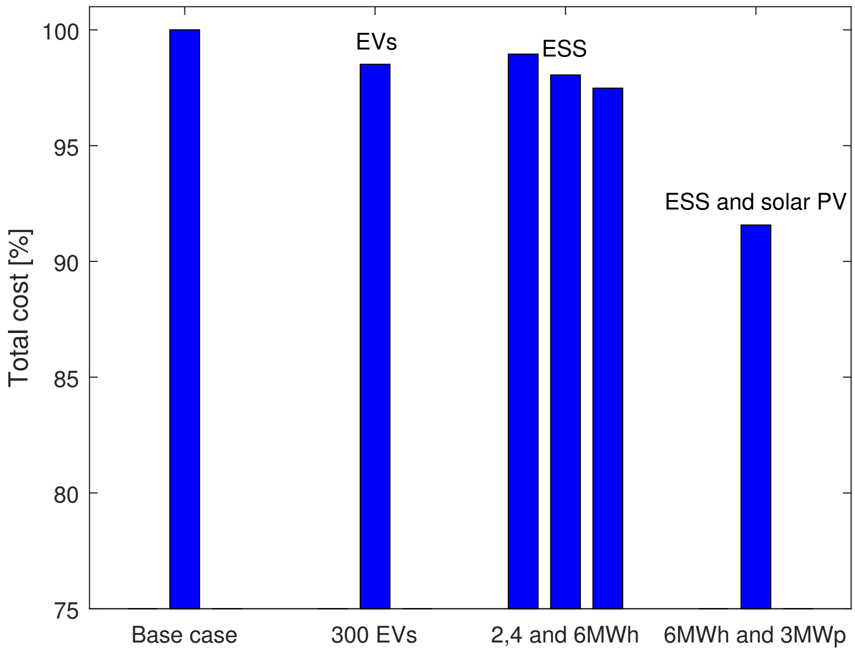

Figure 5.7: Total energy cost compared to base case for different configurations including battery storage, solar power and EVs.

6
Conclusions and Future work

6.1 Conclusions*

This thesis was focused on three different objectives. Firstly, a database of the grid data and load profiles for each bus in the Chalmers microgrid was developed. A load profile for 24 hours was extracted from measurements and then extended to cover an entire year. The second objective was to use the database to create an EMM in order to simulate the grid operating as a microgrid. This model involves local generation, variable loads, fixed loads, grid data and ESS. It was realized using GAMS and the models validity was then confirmed by using PSS/E. The final objective was to use the model in order to observe the benefits by operating the grid as a microgrid. This was accomplished by several case studies where the grid was operated under different circumstances.

- Base case operation when the grid was run as a microgrid was compared to the current operating state. Here, no ESS was available so the benefits originate from scheduling the local generation and the flexible loads. It is shown that the total cost can be lowered by 5700 SEK.
- Part of operating a grid as a microgrid is the ability to run it in island mode. This was implemented and tested for two one-hour outages where the grid was operated independently for one hour. The simulation results shows that with a proper ESS size the grid can withstand a disconnection to the main grid for one hour.
- More renewable energy resources, in the form of solar PV, were implemented in the grid and the benefits were evaluated for different ESS sizes. It was found that the optimal solution was to only invest in solar since the cost of ESS is very high compared to the benefits. However, by only investing in solar PV the ability to operate in island mode is lost due to the unreliable nature of solar power. Therefore, an investment in both solar and ESS is more suitable for this microgrid.
- By using an EV fleet in place of an ESS, the total energy cost can be reduced by approximately 100 000 SEK annually for 300 vehicles. This eliminates the need to invest in additional ESS but the grid infrastructure needs to be further developed to realize this. There is also the matter of battery degradation when using EVs in a microgrid and the owners must therefore be compensated for

*The results from this thesis has been summarized in the paper: "Cost-benefit analysis of battery storage investment for microgrid of Chalmers university campus using OPF framework" shown in appendix A.2

this to be a viable option.

The study shows that there is value in operating the grid as a microgrid and with additional local generation and ESS the total energy cost for the system can be lowered by 8.43% while being able to operate in island mode for a minimum of 1 hour.

6.2 Future Work

- *Linearization of the EMM* - The power flow equations and other constraints are highly non-linear which causes high simulation time. By linearizing constraints the medium-term model could be used for energy storage location studies and also reduce the simulation time overall.
- *Energy storage alternatives* - Further investigation of cheaper alternatives to energy storage and comparisons of investment in storage and local generation could be conducted.
- *Load control in MG* - Investigation of flexible load possibilities could also be interesting since the battery size could be reduced if only critical loads were to be supplied during island mode operation. To gain a more accurate model of when the ventilation power can act as a flexible load, measurements regarding temperature and carbon dioxide in the buildings need to be incorporated in the model. The Ventilation can only be down regulated if the levels of temperature and carbon dioxide are within acceptable limits.
- *Taxes and grid tariff* - Including taxes, peak power cost and fixed grid costs in the model would give a more accurate representation of the energy cost. This could have an impact on how beneficial the ESS would be and how it is utilized.
- *Utilization of CHP* - The usage of the heat distribution from the CHP plant could also be investigated to reduce the cost of operating the plant. As it looks now, all the heat is assumed to be wasted and the cost for electricity production is therefore high. Also ramp-up and ramp-down constraints for the CHP plant needs to be incorporated for a more accurate model.
- *Load profile resolution* - To actually be able to operate Chalmers' grid as a microgrid, the load profile needs to be on a shorter time scale. This needs to be measured on each individual bus, and these kind of measurements does not exist today.

References

[1] G. Pepermans et al., "Distributed generation: definition, benefits and issues." Energy policy, vol. 33, no. 6, pp.787-798, April 2005.

[2] A.A Salam et al., "Technical challenges on microgrids," in ARPN Journal of Engineering and Applied Sciences, vol.3, no. 6, pp. 64-69, December 2008.

[3] Q. Fu et al., "The Role of Energy Storage in a Microgrid Concept: Examining the opportunities and promise of microgrids.," in IEEE Electrification Magazine, vol. 1, no. 2, pp. 21-29, Dec. 2013.

[4] R. H. Lasseter and P. Paigi, "Microgrid: a conceptual solution," 2004 IEEE 35th Annual Power Electronics Specialists Conference (IEEE Cat. No.04CH37551), 2004, pp. 4285-4290 Vol.6.

[5] B. S. Hartono et al., "Review of microgrid technology," QiR (Quality in Research), 2013 International Conference on, Yogyakarta, 2013, pp. 127-132.

[6] J. Marecki "Combined heat & power generating systems," IET; 1988, (Vol.3 pp. 1-2).

[7] X.Tan, Q.Li,H.Wang, "Advances and trends of energy storage technology in Microgrid," International Journal of Electrical Power & Energy Systems, Vol. 44, no 1, pp. 179-191, January 2013.

[8] A. Poullikkas, "A comparative overview of large-scale battery systems for electricity storage," Renewable and Sustainable Energy Reviews, vol. 27, pp.778-788, November 2013.

[9] R.E. Chiez, J.F. Whitacre, "Comparative techno-economic analysis of hybrid micro-grid systems utilizing different battery types," Energy Conversion and Management, Vol. 112, pp. 435-444, March 2016.

[10] B. Nykvist, M- Nilsson, "Rapidly falling costs of battery packs for electric vehicles," Nature Climate Change, Vol 5, no 4, pp. 329-332, 2015.

[11] W. Kempton, J. Tomić, "Vehicle-to-grid power fundamentals: Calculating capacity and net revenue," Journal of power sources, Vol 144, no 1, pp. 268-279, 2005.

[12] W. Kempton, J. Tomić, "Vehicle-to-grid power implementation: From stabilizing the grid to supporting large-scale renewable energy," Journal of power sources, Vol 144, no 1, pp. 280-294, 2005.

[13] B. Bolund, H. Bernhoff, M. Leijon, "Flywheel energy and power storage systems." Renewable and Sustainable Energy Reviews, vol 11, no 2, pp. 235-258, February 2007.

[14] R. Sebastián, RP. Alzola, "Flywheel energy storage systems: Review and simulation for an isolated wind power system," Renewable and Sustainable Energy Reviews, Vol 16, no 9, pp. 6803-6813, December 2012.

[15] I. Hadjipaschalis, A. Poullikkas, V. Efthimiou, "Overview of current and future energy storage technologies for electric power applications," Renewable and sustainable energy reviews, vol 13, no 6, pp. 1513-1522, September 2009.

[16] D. Steen., "Modelling of Demand Response in Distribution Systems." Ph.D. dissertation, Dept of Energy and Environment, Chalmers University of Technology, Gothenburg, Sweden, 2014.

[17] A. Oudalov, R. Cherkaoui and A. Beguin, "Sizing and Optimal Operation of Battery Energy Storage System for Peak Shaving Application," Power Tech, 2007 IEEE Lausanne, Lausanne, 2007, pp. 621-625.

[18] Su, Wencong, and Jianhui Wang. "Energy management systems in microgrid operations," The Electricity Journal, vol. 25, no 8, pp.45-60, October 2012.

[19] S. X. Chen et al., "Sizing of Energy Storage for Microgrids," in IEEE Transactions on Smart Grid, vol. 3, no. 1, pp. 142-151, March 2012.

[20] C. Chen et al., "Optimal Allocation and Economic Analysis of Energy Storage System in Microgrids," in IEEE Transactions on Power Electronics, vol. 26, no. 10, pp. 2762-2773, Oct. 2011.

[21] N.W.A Lidula, A.D Rajapakse, "Microgrids research: A review of experimental microgrids and test systems," Renewable and Sustainable Energy Reviews,Vol 15, no 1, pp. 186-202, 2011.

[22] R.Lasseter, A.Khalsa. (2016, May 13). *CERTS Microgrid Test Bed* [Online]. Availible: https://certs.lbl.gov/initiatives/certs-microgrid-test-bed

[23] G. Turner, J. P. Kelley, C. L. Storm, D. A. Wetz and W. J. Lee, "Design and Active Control of a Microgrid Testbed," in IEEE Transactions on Smart Grid, vol. 6, no. 1, pp. 73-81, Jan. 2015.

[24] R. M. González, T. A. J. van Goch, M. F. Aslam, A. Blanch and P. F. Ribeiro, "Microgrid design considerations for a smart-energy university campus," IEEE PES Innovative Smart Grid Technologies, Europe, Istanbul, 2014, pp. 1-6.

[25] M. Meiqin, S. Shujuan and L. Chang, "Economic analysis of the microgrid with multi-energy and electric vehicles," 8th International Conference on Power Electronics - ECCE Asia, Jeju, 2011, pp. 2067-2072.

[26] E. Hossain, E. Kabalci, R. Bayindir , R. Perez, "Microgrid testbeds around the world: State of art," Energy Conversion and Management, vol 86, pp.132-153, October 2014.

[27] Elsayed et al., "DC microgrids and distribution systems: An overview." in Electric Power Systems Research, vol.119, pp. 407-419, February 2015.

[28] X. Liu, P. Wang and P. C. Loh, "A Hybrid AC/DC Microgrid and Its Coordination Control," in IEEE Transactions on Smart Grid, vol. 2, no. 2, pp. 278-286, June 2011.

[29] Justo, Jackson John, et al. "AC-microgrids versus DC-microgrids with distributed energy resources: A review," Renewable and Sustainable Energy Reviews, vol. 24, pp.387-405, August 2013.

[30] *Nordpool web page* (2016, May 27) [Online].
Available: http://www.nordpoolspot.com/

[31] *International Electrotechnical Commission. Photovoltaic devices—Part 3: measurement principles for terrestrial photovoltaic (PV) solar devices with reference spectral irradiance data.* IEC 60904–3 ed2, 2008

[32] *GAMS web page* (2016, September 16) [Online].
Available: http://www.gams.com/

[33] *Model S Specifications* (2016, Aug 31) [Online].
Avalible: https://www.tesla.com/support/model-s-specifications?redirect=no

[34] Mayer JN, Simon P, Philipps NS, Schlegl T, Senkpiel C. "Current and future cost of photovoltaics," Long-term Scenarios for Market Development, System Prices and LCOE of Utility-Scale PV Systems (Fraunhofer ISE, Study on behalf of Agora Energiewende, Freiburg, 2015). 2015 Mar.

A

Appendix 1

A.1 GAMS Code

```
*Defining sets
set i buses /1*41/;
alias(i,j);
set h hour;
set d(h) daytime;
set Head2   Line data table headings / Re, Xe, Ch /;

*Parameter definitions
$parameter P_load(i,h) load at bus i and hour h;$
$parameter Q_load(i,h) img load at bus i and hour h;$
$parameter Elprice(h) electricity cost at hour h;$
$parameter Pmax(i) max Pgen at bus i /13 inf, 16 1/;$
$parameter Qmax(i) max Qgen at bus i /13 inf, 16 0.3/;$
$parameter Pemax(i);$
$parameter Ilim(i,j);$
$parameter Pfan(i,h);$
$parameter Psolar(i,h);$

*Scalar definitions
scalar Emax;
scalar phi            /3.141592654 /;
scalar Sbase     base in MVA     /1/;
scalar CostCHP   SEK per MW    /600/;
scalar chr       efficiency of energy storage /0.95/;
scalar dis       efficiency of energy storage /0.95/;


*Input data loaded from MATLAB code
\$GDXIN Z:\.win\Desktop\GAMS\1year_model.gdx
\$LOAD h=Hour
\$LOAD d=Daytime
\$LOAD Elprice=Elspot
\$LOAD P_load=Load_real
\$LOAD Q_load=Load_img
```

```
\$LOAD Pemax=Pemax
\$LOAD Emax=E_max
\$LOAD Ilim=I_lim
\$LOAD Pfan=Pfan
\$LOAD Psolar=Psolar
\$GDXIN

display Elprice,P_load,Q_load,Pemax,Emax;


*Line data for the grid in p.u, used to form an admittance matrix
Table LineData(i,j,Head2)
                 Re            Xe          Ch
1.2       0.0000000     0.0208110     0.00000
1.3       0.0000853     0.0000580     0.00100
1.5       0.0000798     0.0000535     0.00097
3.4       0.0000000     0.0737500     0.00000
5.6       0.0000635     0.0000308     0.00048
5.12      0.0003120     0.0002113     0.00380
5.41      0.0001306     0.0000580     0.00085
6.7       0.0000000     0.0580000     0.00000
8.9       0.0000000     0.0725000     0.00000
8.17      0.0001252     0.0000844     0.00150
10.11     0.0000000     0.0602500     0.00000
10.41     0.0001868     0.0000825     0.00120
12.13     0.0000145     0.0000010     0.00017
12.16     0.0000172     0.0000118     0.00021
12.17     0.0000227     0.0000154     0.00028
12.18     0.0000281     0.0000190     0.00035
13.14     0.0004762     0.0003229     0.00580
14.15     0.0000000     0.0132430     0.00000
16.19     0.0000281     0.0000190     0.00035
17.31     0.0003746     0.0002540     0.00460
17.33     0.0000907     0.0000617     0.00110
18.22     0.0000000     0.0440000     0.00000
18.23     0.0002549     0.0001732     0.00310
18.35     0.0004535     0.0003075     0.00550
19.20     0.0000000     0.0223170     0.00000
23.24     0.0000000     0.1067500     0.00000
23.25     0.0003401     0.0002304     0.00420
25.26     0.0000000     0.0600000     0.00000
25.27     0.0001868     0.0001270     0.00230
27.28     0.0000000     0.0612500     0.00000
29.30     0.0000000     0.0725000     0.00000
29.35     0.0004653     0.0003156     0.00570
31.32     0.0000000     0.0360000     0.00000
```

```
33.34     0.0000000     0.0393750     0.00000
35.36     0.0000000     0.0361930     0.00000
35.38     0.0000118     0.0000082     0.00014
38.39     0.0000363     0.0000109     0.00012
39.40     0.0000000     0.0208000     0.00000
41.21     0.0000000     0.0334360     0.00000
;

*Admittance matrix
Parameter Z(i,j), GG(i,j), BB(i,j), YCL(i);
Parameter G(i,j), B(i,j), Y(i,j), ZI(i,j), Theta(i,j);

LineData(j,i,"Re")$(LineData(i,j,"Re") gt 0.00) = LineData(i,j,"Re");
LineData(j,i,"Xe")$(LineData(i,j,"Xe") gt 0.00) = LineData(i,j,"Xe");
LineData(j,i,"Ch")$(LineData(i,j,"Ch") gt 0.00) = LineData(i,j,"Ch");

Z(i,j) = (LineData(i,j,"Re"))**2 + (LineData(i,j,"Xe"))**2 ;
GG(i,j)$(Z(i,j) ne 0.00) = LineData(i,j,"Re")/z(i,j) ;

BB(i,j)$(Z(i,j) ne 0.00) = -LineData(i,j,"Xe")/Z(i,j);
BB(j,i)$(Z(i,j) ne 0.00) = -LineData(i,j,"Xe")/Z(i,j);

YCL(i) = sum(j, LineData(i,j,"Ch"));

B(i,i) = sum(j, BB(i,j)) + YCL(i);
G(i,i) = sum(j, GG(i,j));
G(i,j)$(ord(i) ne ord(j)) = -GG(i,j);
B(i,j)$(ord(i) ne ord(j)) = -BB(i,j);

Y(i,j) = sqrt(G(i,j)*G(i,j) + B(i,j)*B(i,j));

ZI(i,j)$(G(i,j) ne 0.00)  = abs(B(i,j))/abs(G(i,j));

Theta(i,j) = arctan(ZI(i,j));
Theta(i,j)$((B(i,j) eq 0) and (G(i,j) gt 0)) = 0.0;
Theta(i,j)$((B(i,j) eq 0) and (G(i,j) lt 0))   = -0.5*phi;
Theta(i,j)$((B(i,j) gt 0) and (G(i,j) gt 0))   = Theta(i,j);
Theta(i,j)$((B(i,j) lt 0) and (G(i,j) gt 0))   = 2*phi - Theta(i,j);
Theta(i,j)$((B(i,j) gt 0) and (G(i,j) lt 0))   = phi - Theta(i,j);
Theta(i,j)$((B(i,j) lt 0) and (G(i,j) lt 0))   = phi + Theta(i,j);
Theta(i,j)$((B(i,j) gt 0) and (G(i,j) eq 0))   = 0.5*phi;
Theta(i,j)$((B(i,j) lt 0) and (G(i,j) eq 0))   = -0.5*phi;
Theta(i,j)$((B(i,j) eq 0) and (G(i,j) eq 0))   = 0.0 ;

Display Y, Theta
```

```
*Variable definitions
VARIABLES
Q(i,h) Reactive power generation at bus i and hour h
P(i,h) Active power generation at bus i and hour h
V(i,h) Voltage at bus i and hour h
Cost Total system cost
Loss Total system transmission losses
Delta(i,h) Voltage angle in radians
SOC(i,h) State of charge at bus i
Pec(i,h) Charge power from ESS at bus i and hour h
Ped(i,h) Discharge power from ESS at bus i and hour h
Revenue Total revenue of storage
ReI(i,j,h) Real part of current between bus i and j at hour h
ImI(i,j,h) Imaginary part of current between bus i and j at hour h
Pflex(i,h) Amount of flexible load at bus i and hour h
Qbatt(i,h) Reactive power from batteries at bus i and hour h
Iabs(i,j,h) Absolute current
;


*Equation definitions
EQUATIONS
CostFn       Total system generation cost in $
Equn1(i,h)     Real power load flow equation
Equn2(i,h)     Reactive power load flow equation
SOC1(i,h)      SOC equation
SOC2(i,h)      SOC equation
Totgen(h)      Total power generated
Totrev         Total revenue
RI(i,j,h)      Real part of current between buses
II(i,j,h)      Imaginary part of current between buses
Flexeq(i,h)    Equation to limit load curtailment
ChargeEq(i,h)  Charge equation
Itot(i,j,h)    Absolute current
Ili    Current limitation equation
Ili2    Current limitation equation
;



*Constraints on variables
V.up(i,h) = 1.05;
V.lo(i,h) = 0.95;

Q.up(i,h) = Qmax(i);
```

```
P.up(i,h) = Pmax(i);


Pflex.lo(i,h) = 0;
Pflex.up(i,h) = 0;
Pflex.up(i,d)= 0.2*Pfan(i,d);


Qbatt.up(i,h) = 0.3*Pemax(i);
Qbatt.lo(i,h) = -0.3*Pemax(i);


SOC.up(i,h) = 1;
SOC.lo(i,h+1)$(Pmax('13') gt 0) = 6/Emax;
SOC.lo(i,h+1)$(Pmax('13') eq 0) = 0;
SOC.fx(i,'1')$(Pemax(i) ne 0) = 6/Emax;


Pec.up(i,h) = Pemax(i);
Pec.lo(i,h) = 0;
Ped.up(i,h) = Pemax(i);
Ped.lo(i,h) = 0;

*Equation limiting to load curtailment
Flexeq(i,h)$(ord(h) ne card(h)).. Pflex(i,h)*Pflex(i,h+1)*10000000 =e= 0;

*Load flow equations
Equn1(i,h).. P(i,h) - P_load(i,h) + dis*Ped(i,h) - Pec(i,h) + Psolar(i,h) +
Pflex(i,h) =e= Sum(j, Y(i,j)*V(i,h)*V(j,h)*Cos(theta(i,j) + Delta(j,h) -
Delta(i,h)));
Equn2(i,h).. Q(i,h) - Q_load(i,h) + Qbatt(i,h) + tan(arccos(0.98))*Pflex(i,h)
=e= -Sum(j, Y(i,j)*V(i,h)*V(j,h)*Sin(theta(i,j) + Delta(j,h) - Delta(i,h)));

*SOC equations
SOC1(i,h)$(ord(h) ne 1).. SOC(i,h) =e= SOC(i,h-1)+chr*Pec(i,h-1)/(Emax)-
Ped(i,h-1)/(Emax);
SOC2(i,h)$(ord(h) eq card(h)).. Pe(i,h) =e= (SOC(i,h)-SOC.lo(i,h))*Emax;

*Charge equation
ChareEq(i,h).. Pec(i,h)*Ped(i,h) =e= 0;

*Calculation of revenue
TotRev.. Revenue =e= sum((i,h),Pe(i,h)*Elprice(h))*Sbase;

*Equations for line constraints
```

```
RI(i,j,h).. ReI(i,j,h) =e=
V(j,h)*Y(i,j)*COS(Theta(i,j)+Delta(j,h)) -
V(i,h)*Y(i,j)*COS(Theta(i,j)+Delta(i,h)) +
V(i,h)*LineData(i,j,"ch")*SIN(Delta(i,h));

II(i,j,h).. ImI(i,j,h) =e= V(j,h)*Y(i,j)*SIN(Theta(i,j)+Delta(j,h))
- V(i,h)*Y(i,j)*SIN(Theta(i,j)+Delta(i,h)) +
 V(i,h)*LineData(i,j,"ch")*COS(Delta(i,h));

Itot(i,j,h).. Iabs(i,j,h) =e= sqrt(power(ReI(i,j,h),2) + power(ImI(i,j,h),2));

Ili(i,j,h).. Iabs(i,j,h) =l= Ilim(i,j);
Ili2(i,j,h).. Iabs(i,j,h) =g= -Ilim(i,j);


*Objective function - Total cost
CostFn.. Cost =e= (sum(h,P('13',h)*Elprice(h)+P('16',h)*CostCHP)+
sum((i,h),Pflex(i,h)*240))*Sbase;

*Model formulation describing which equations are included in the model
model OPF /
Equn1
Equn2
CostFn
ChargeEq
SOC1
SOC2
Totrev
Flexeq
RI
II
Itot
Ili
Ili2
/;


*Solve statement
solve OPF using NLP minimizing Cost;


*Output data to MATLAB
execute_unload 'results',Cost,SOC,Pec,Ped,Revenue;
```

A.2 Summarized paper

Cost-benefit analysis of battery storage investment for microgrid of Chalmers university campus using OPF framework

Martin Göransson, Niklas Larsson and Le Anh Tuan
Department of Energy and Environment
Chalmers University of Technology
Gothenburg, Sweden
Email: tuan.le@chalmers.se

***Abstract*—This paper presents a cost-benefit approach for evaluation of battery energy storage (BES) options to be installed in the electrical distribution grid of Chalmers University from the microgrid perspective. The evaluation is based on a multi-period ac optimal power flow (OPF) model applied for microgrid, which is referred to as the μ-OPF, with the objective function being the total grid operation cost. The model is developed for the real 12 kV grid of Chalmers. The μ-OPF is used as the calculation tool for the cost-benefit analysis where the benefit-to-cost ratios (BCR) of battery options in the grid in a year over the annualized cost of battery are evaluated for various options of battery placements in the grid. The BCRs demonstrate the cost-effectiveness of the battery in microgrid operation. Battery options considered include both distributed option and a centralized option. It has been found that the optimal location of battery storage at Chalmers grid is at the point of connection to upstream grid of Gothenburg Energy distribution system. The study results show that the benefit gained from using battery storage increases with the size of battery, and the size with the highest BCR was found to be 2 MWh when considering the grid-connected mode of operation. The optimal size when the grid is in island mode is however dependent on island mode capability.**

***Index Terms*—Microgrid, Battery energy storage (BES), Flexible demand, Solar PV, Cost-benefit analysis, University Campus**

NOMENCLATURE

$Sets$	
H	Total number of hours in the simulation time-horizon
K	Total number of buses in the microgrid
$Indices$	
h	Hour
d	Hour during day-time
i, j	Indices for buses
$Variables$	
TC	Total grid operation cost
P_h^{grid}	Power from the main grid
P_h^{CHP}	Power from the combined heat and power (CHP) plant
$\Delta P_{i,h}^{load}$	Active load curtailment
$\Delta Q_{i,h}^{load}$	Reactive load curtailment
$P_{i,h}^{gen}$	Active power generation at bus i and hour h
$Q_{i,h}^{gen}$	Reactive power generation at bus i and hour h
V	Voltage magnitude
I	Current magnitude
SOC	State of charge of battery
$P_{i,h}^{ec}$	Active power to battery storage during charging
$P_{i,h}^{ed}$	Active power from battery storage during discharging
$Q_{i,h}^{BES}$	Reactive power from battery storage
$E_{i,h}$	Stored energy at bus i for hour h
$Parameters$	
E_i^{rated}	Installed battery energy storage at bus i
$B_{i,j}$	Imaginary element of the admittance matrix
$G_{i,j}$	Real element of the admittance matrix
C_h^{grid}	Cost to buy power from main grid
G^{CHP}	Unit generation cost of the CHP plant
PF	Penalty factor for load curtailment
$P_{i,d}^{fan}$	Total fan load for bus i and hour d
$P_{i,h}^{load}$	Active power load at bus i and hour h
$Q_{i,h}^{load}$	Reactive power load at bus i and hour h
V_i^{min}	Minimum voltage magnitude
V_i^{max}	Maximum voltage magnitude
$I_{i,j}^{lim}$	Maximum current limit on line i-j
eff^{chr}	Charging efficiency of battery storage
eff^{dis}	Discharging efficiency of battery storage

I. INTRODUCTION

The increasing penetration of small-scale distributed energy resources (DERs), including wind power, solar photovoltaics (PV), micro combined heat and power (CHP) units, etc. and the electric vehicles (EVs) in the distribution system put a quite challenging task to the distribution system operator to control and operate the system in a reliable manner. The microgrid concept has been introduced to partially address this challenge [1]. A microgrid is generally defined as a local cluster with a clear geographical boundary within a

The work presented in this paper is partly funded by Energy Area of Advance of Chalmers University of Technology.

distribution system, which can coordinate the operation of DERs and energy storage to supply the local load demand in an economic and reliable manner [2], [3]. Microgrids offer both technical and economic benefits to the distribution system operators. With many microgrids developed, the control of DERs in the distribution system can be passed on to the local control in the microgrids. Microgrids can be operating in grid-connected as well as off-grid (island) modes. Microgrids thus help to utilize the DERs to their fullest extent. Customers within microgrid would expect to have more reliable electricity supply service, thanks to the capability to operate in both modes. The distribution system will benefit from microgrid since it will minimize the peak power demand in the distribution system, reduce the need for power transmission, and thus increase the overall efficiency.

Microgrid development has recently been taking place at several university campus environment, including Eindhoven university of technology [4], university of Genoa [5], [6]. The common goals for these university campuses' microgrid are to improve the economic performance of the grid and to reduce the use of fossil-based generation. Chalmers University of Technology has identified microgrid as one of its strategic research areas. One of the projects in microgrid which has recently received funding from EU Urban Innovative Action program [9] would focus on transformaing electrical grid of Chalmers University of Technology into an intelligent microgrid which can be used as microgrid test bed. This test bed will support investigations of methods and strategies for design, control, protection, operation of microgrids. The aim is also to demonstrate a concept of fossil-free energy district in modern urban context. As a first step in this project, an initial investigation of microgrid design has to be perform. One of the tasks in this step is to identify the optimal placement of battery energy storage (BES) within the microgrid.

Energy storage is an important component in a microgrid, which can be used for demand response, storing excess energy and support island mode operation. Cost-benefit analysis is one of common approaches to evaluate the cost-effectiveness of the investment which can be applied for the case of battery energy storage in microgrid. A number of work has been presented in this topic. The most relevant work was found in [7] in which a method for choosing the optimal size was developed based on a cost-benefit analysis for both islanded and grid connected microgrids. The total benefits are calculated for values between a chosen minimum and maximum energy storage size in order to obtain the most beneficial size. However, constraints on physical electrical grid were not considered. Also, the model used is only for 24-hour period. This present paper proposed a cost-benefit analysis which is based on a multi-period optimal power flow model built on the one developed in [8] with detailed ac load flow constraints and the model is applied for the whole year (8760 hours) to evaluate the benefit of different candidates of battery storage. The main contributions of this present paper can be summarized below:

- *Development of the grid model*: Data for Chalmers' internal electrical distribution grid was not readily available for grid simulation. This data has been acquired through different methods and used for simulating the grid. Also, collection and evaluation of whole-year demand profiles at building levels and solar generation data of Chalmers campus has been made.
- *Development of μ-OPF model*: The μ-OPF model for Chalmers microgrid was developed with the objective function being the total grid operation cost (i.e., cost of energy imported which is considered to be dependent of the spot price electricity plus the cost of own production from the CHP plant). Technical constraints in the models include power flow constraints, battery state of charge limits, as well as other constraints of flexible demands in the grid. A simulation platform was created using GAMS [10] as the modeling and optimization tool and MATLAB [11] for data handling and automation.
- *Proposed cost-benefit analysis for BES*: The paper has proposed to use cost-benefit analysis approach based on μ-OPF model for 1-year simulation study period to evaluate the battery energy storage candidates which can reflect the variations in load and solar energy as well as weather conditions over the whole year.

II. Development Chalmers' Distribution Grid Model And Database

A. Grid data

The internal electrical grid at Chalmers is used to distribute power to the campus and consists of 22 buses where 17 are load buses and can be seen in Fig. 1. Akademiska Hus [12] provided data of cables and transformers, from which a load flow model of Chalmers grid has been implemented.

B. Load profile and flexible demand

Demand profiles for each bus (i.e., building) in the grid have been extracted based on current (I) measurements by the ABB Micro-SCADA system and energy demand for each building provided by Akademiska Hus [12]. The current (I) measurements are extracted and stored for every 10-minute interval with a backlog for only 24 hours. Therefore, a scaling factor based on the energy consumption was used to approximate the demand profile for one year. A load profile was measured for a day in March 2016, with peak load of 5.5 MW at hour 14. The total power demand at Chalmers varies between 2.5 and 7.0 MW and the annual energy consumption is 32000 MWh. The main loads in the campus include e.g., lighting, computers, ventilation, and electric machines in laboratories. There are a number of EVs currently in use in the campus which represents distributed BES.

Flexible demand due to adjustments in the ventilation power within building in Chalmers grid is possible to a certain extent. The ventilation power is a total of 500 kW spread out over the campus and can be reduced temporarily by 20%. This load reduction can only occur during the day-time, between when the ventilation is operating at maximum capacity and only for one hour at a time so that the working environment remains comfortable. Activation of the load curtailment is assumed

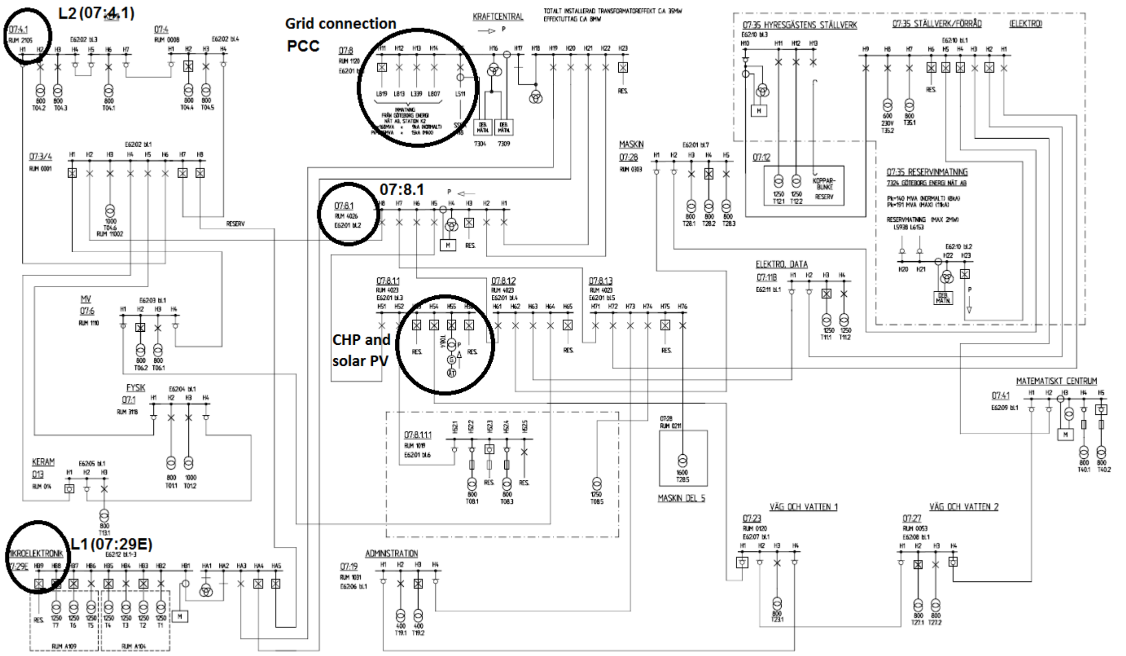

Fig. 1. Single line diagram of Chalmers 12kV electrical distribution grid

to occur when the energy cost exceeds 20% of the mean electricity price for 2015 which is at 240 SEK/MWh, seen as a fictive cost paid by the grid operator when the load is reduced.

C. *Own generation*

Currently there are three sources for electric power in the internal grid, generated by a CHP unit, from solar PV and power bought from the main grid with prices from Nordpool day ahead market [13]. The CHP unit can produce up to 1 MW at a cost of 600 SEK/MWh [12]. Solar PV panels are installed on a wall of one of the buildings on campus and are assumed to produce energy with no cost. This energy is calculated based on the rating of 15.7 kW and the irradiance data for Gothenburg obtained from System Advisor Model (SAM) [14].

III. Methodology For Cost-benefit Analysis

To evaluate which BES configuration yields the highest cost-benefits ratio, different locations and sizes of BES were investigated using the μ-OPF, which is described in the next section. The flowchart shown in Fig. 2 shows how the comparison between cases is performed and evaluated. The evaluation is based on a cost-benefit analysis for all cases except the location. The location was instead determined based on the losses in the system to establish how the BES location affects the grid operations. The simulations are based on a time-resolution of one hour. When one year simulations are performed, the simulation is split into 12 separate simulations corresponding to 12 months of the year in order to reduce simulation time.

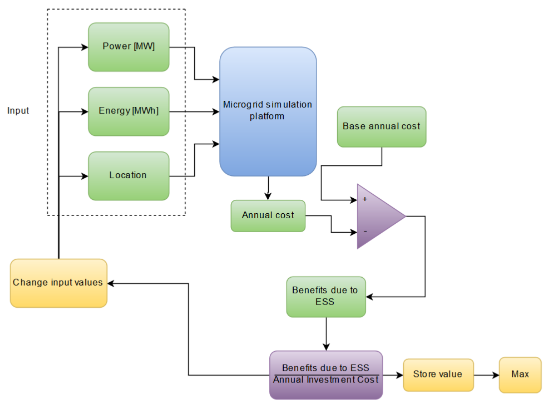

Fig. 2. Methodology for determining the optimal BES based on a cost-benefit analysis

IV. Formulation Of Optimal Power Flow Model Of Chalmers' Microgrid

This section presents the main equations of Chalmers microgrid μ-OPF model.

- *Objective function*: The objective of the model is to minimize the total operation cost of the system including the cost of energy import, cost of own production as well as the cost of demand control.

$$TC = \sum_{h \in H} \sum_{i \in K} P_h^{CHP} C^{CHP} + P_h^{grid} C_h^{grid} + PF \Delta P_{i,h}^{load} \quad (1)$$

- *Power flow equations with battery storage and flexible demand*:

$$P_{i,h}^{gen} - P_{i,h}^{load} + P_{i,h}^{ec} - eff^{dis} * P_{i,h}^{ed} + \Delta P_{i,d}^{load} = \sum_{j \in K} |V_i||V_j|(G_{i,j} \cos\theta_{i,j} + B_{i,j} \sin\theta_{i,j}) \quad (2)$$

$$Q_{i,h}^{gen} - Q_{i,h}^{load} + Q_{i,h}^{BES} + \Delta Q_{i,d}^{load} = \sum_{j \in K} |V_i||V_j|(G_{i,j} \cos\theta_{i,j} - B_{i,j} \sin\theta_{i,j}) \quad (3)$$

The voltage magnitudes, V_i, and current magnitudes, $I_{i,j}$, are limited according to (4) and (5).

$$V_i^{min} \leq V_i \leq V_i^{max} \quad (4)$$

$$|I_{i,j}| \leq I_{i,j}^{lim} \quad (5)$$

where, V_i^{min} and V_i^{max} are the minimum and maximum voltage levels and $I_{i,j}^{lim}$ is the maximum allowed current between bus i and j.

- *Flexible demand constraints*:
Installed ventilation power is currently 500 kW and can be reduced by 20 % when desired according to (6).

$$\Delta P_{i,d}^{load} \leq 0.2 * P_{i,d}^{fan} \quad (6)$$

The frequency at which the load curtailment occurs is limited to every other hour as seen in (7).

$$\Delta P_{i,d}^{load} * \Delta P_{i,d+1}^{load} = 0 \quad (7)$$

- *Battery energy storage constraints*:
The BES is modeled as either a charging or discharging power. Monitoring is done by observing the state of charge (SOC), which is defined by (8) and limited by (9).

$$SOC_{i,h} = \frac{E_{i,h}}{E_i^{max}} \quad (8)$$

$$0 \leq SOC_{i,h} \leq 1 \quad (9)$$

Variations of the SOC over the simulation period is calculated as seen in (10). Since the model uses a one hour data resolution the power utilized by the BES can be compared to the energy capacity of the BES.

$$SOC_{i,h} = SOC_{i,h-1} + \frac{eff^{chr} * P_{i,h-1}^{ec}}{E_i^{rated}} - \frac{P_{i,h-1}^{ed}}{E_i^{rated}} \quad (10)$$

The μ-OPF model is of non-linear programming type. It has been implemented in GAMS environment [10] and solved using MINOS solver [15].

V. Summary Of Study Results

This section presents preliminary results of the paper including optimal location for BES and total benefits for different sizes of BES for a 1-year period. In the full version of the paper, the following results will be discussed and presented:

- Optimal configuration of BES, including location and size, based on a cost-benefit analysis and island mode capabilities.
- Energy scheduling during island mode operation
- A more accurate load profile including different load within each building to establish more flexible loads
- Sensitivity analysis of benefits of storage with respect to changes in capacity of local generation, solar PVs, and prices of battery storage.

Different aspects of the BES were varied to achieve an optimal configuration with regards to the total energy cost and island mode capabilities. Four different locations for connection of battery storage were investigated for both an aggregated and a distributed BES, yielding a total of eight cases which where evaluated regarding the line losses. The considered connection point for BES are shown by the circles in Fig. 1. Those include point of common coupling (PCC) (i.e., the main grid connection point), the two most heavily loaded buses (L1 and L2) to enable the highest loads to be efficiently supplied. The introduction of BES at the high load buses would further increase the load when the batteries are charged, however the batteries are charged during low price hours which correlates to the hours with lower demand. Finally, bus 07:8.1 was also investigated. These simulations have been carried out for a time span of 24 hours with a total installed BES size of 6 MWh.

TABLE I
BES LOCATION COMPARISON

Location	Loss [kW]
PCC	40
PCC, 07:8.1	41
PCC, 07:8.1, L1, L2	43
07:8.1	43
PCC, L1	46
PCC, L2	48
L1	69
L2	75

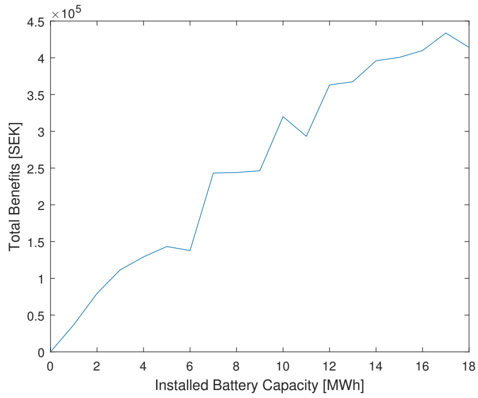

Fig. 3. Total benefits for different BES capacities

As shown in Table I, the configuration which yields the lowest losses is to place the entire BES at the PCC which is used for all further simulations. The worst cases are to have the BES entirely at L1 or L2, due to the higher loading on the lines during charging and discharging of the BES.

When the microgrid is operated in grid-connect mode, the BES is used for demand response by charging when the energy price is low and discharging when the price is high. This will reduce the total energy cost which is a benefit to the microgrid operator (Akademiska Hus in this case). The total benefit for different BES sizes has been shown in Fig. 3. It can be seen from the figure that total benefits increase as the BES capacity increases, however at a decreasing rate. This means that it might not be beneficial to invest in more storage than necessary for the desired island mode operation time.

Operation in island mode is possible when an BES is installed with enough capacity to supply the demand, together with local generation, for the duration of an outage due to fault in the upstream grid. During that time, the BES is supplying the demand together with the local generation and being recharged during the succeeding hours to be ready for another possible outage.

VI. Conclusions

This section presents preliminary conclusions from the work. More concrete conclusions will be made in the full version of the paper.

In this paper, a multi-period optimal power flow model for microgrid has been developed using the real data from the electrical distribution grid of Chalmers university campus. The model has been used in the pre-design phase of microgrid for Chalmers to evaluate cost-effectiveness of the battery storage options. It has been found that the operation of Chalmers as a microgrid as scheduled by the μ-OPF model for the operation of battery storage, demand responses as well as own generation would reduce the total operation cost as well as the total energy loss in the grid. The optimal battery storage option has been suggested based on the highest benefit-to-cost ratio obtained over the whole year. It was shown in the study that the benefit from battery has not outweighed its investment cost, given the high market price of the battery storage at the present. It can be expected that the price of the battery storage will go further down in the future which will improve the cost-effectiveness of the battery. In this study, the battery storage has only been considered for supplying energy in Chalmers microgrid, consideration of other use of battery storage, such as grid support services to the distribution system and power balancing services could further enhance the battery cost-effectiveness. This is however the subject of further study.

Acknowledgment

The authors would like to thank Per Löveryd, Richard Block and their colleagues at Akademiska Hus for providing the data of Chalmers' grid. Thanks are also extended to David Steen at Chalmers for his discussions and support with the work.

References

[1] Hatziargyriou, N.; Asano, H.; Iravani, R.; Marnay, C., "Microgrids," in IEEE Power and Energy Magazine, vol.5, no.4, pp.78-94, July-Aug. 2007.
[2] Parhizi, S.; Lotfi, H.; Khodaei, A.; Bahramirad, S., "State of the Art in Research on Microgrids: A Review," in Access, IEEE , vol.3, no., pp.890-925, 2015
[3] Eklas Hossain, Ersan Kabalci, Ramazan Bayindir, Ronald Perez, Microgrid testbeds around the world: State of art, Energy Conversion and Management, Volume 86, October 2014, Pages 132-153, ISSN 0196-8904,
[4] R. Morales Gonzalez, T. A. J. van Goch, M. F. Aslam, A. Blanch, and P. F. Ribeiro, "Microgrid design considerations for a smart-energy university campus," *IEEE PES Innovative Smart Grid Technologies, Europe*, Oct. 2014.
[5] S. Bracco, F. Delfino, F. Pampararo, M. Robba, and M. Rossi, "The university of Genoa smart polygeneration microgrid test-bed facility: The overall system, the technologies and the research challenges," *Renewable and Sustainable Energy Reviews*, vol. 18, pp. 442459, Feb. 2013.
[6] S. Bracco, F. Delfino, F. Pampararo, M. Robba, and M. Rossi, "Economic and environmental performances quantification of the university of Genoa smart Polygeneration Microgrid," *2012 IEEE International Energy Conference and Exhibition (ENERGYCON)*, Sep. 2012.
[7] S. X. Chen, H. B. Gooi, and M. Q. Wang, "Sizing of energy storage for Microgrids," *IEEE Transactions on Smart Grid*, vol. 3, no. 1, pp. 142151, Mar. 2012.
[8] W. Feng, L. A. Tuan, L. B. Tjernberg, A. Mannikoff and A. Bergman, "A New Approach for Benefit Evaluation of Multiterminal VSCHVDC Using A Proposed Mixed AC/DC Optimal Power Flow," in IEEE Transactions on Power Delivery, vol. 29, no. 1, pp. 432-443, Feb. 2014.
[9] *Urban Innovative Actions web page* (2016) [Online]. Available: http://www.uia-initiative.eu/en
[10] General Algebraic Modeling System (GAMS) *Version 23.9.5*. Washington, DC: GAMS Development Corporation., 2012.
[11] MATLAB, *Version R2014b*. Natick, Massachusetts: The MathWorks Inc., 2014.
[12] *Akademiska Hus web page* (2016) [Online]. Available: http://www.akademiskahus.se/en/
[13] *Nordpool web page* (2016, May 27) [Online]. Available: http://www.nordpoolspot.com/
[14] System Advisor Model (SAM) *Version 2016.3.14* Washington, DC: National Renewable Energy Laboratory., 2016.
[15] MINOS solver manual, [Online]. Available: https://www.gams.com/

A.3 Load Profile

Table A.1: Load profile for each hour of a day, 17/3-2016

Hour	Load [kW]
1	3519.5
2	3521.8
3	3534.6
4	3546.7
5	3579.3
6	3672.9
7	4206.0
8	4679.3
9	5059.4
10	5325.9
11	5367.7
12	5413.9
13	5454.8
14	5472.9
15	5461.4
16	5293.8
17	4884.0
18	4545.5
19	4215.7
20	3974.8
21	3817.5
22	3718.3
23	3610.5
24	3534.2

Hour Bus Nr	1	2	3	4	5	6	7	8	9	10	11	12
1	0.0	0.0	0.0	0.0	0.0	0.0	0.0	0.0	0.0	0.0	0.0	0.0
2	601.0	604.6	604.4	595.2	594.6	608.5	635.0	688.1	759.3	821.7	856.1	879.4
3	0.0	0.0	0.0	0.0	0.0	0.0	0.0	0.0	0.0	0.0	0.0	0.0
4	200.3	201.5	201.5	198.4	198.2	202.8	211.7	229.4	253.1	273.9	285.4	293.1
5	0.0	0.0	0.0	0.0	0.0	0.0	0.0	0.0	0.0	0.0	0.0	0.0
6	0.0	0.0	0.0	0.0	0.0	0.0	0.0	0.0	0.0	0.0	0.0	0.0
7	103.6	103.6	103.6	103.6	103.6	104.0	106.4	111.5	120.7	121.1	121.6	120.9
8	0.0	0.0	0.0	0.0	0.0	0.0	0.0	0.0	0.0	0.0	0.0	0.0
9	138.2	138.2	138.2	138.2	146.9	173.6	190.9	231.8	242.7	255.8	244.6	241.9
10	0.0	0.0	0.0	0.0	0.0	0.0	0.0	0.0	0.0	0.0	0.0	0.0
11	9.8	9.8	9.7	9.8	9.7	9.7	13.0	26.7	35.2	39.7	41.4	43.0
12	0.0	0.0	0.0	0.0	0.0	0.0	0.0	0.0	0.0	0.0	0.0	0.0
13	0.0	0.0	0.0	0.0	0.0	0.0	0.0	0.0	0.0	0.0	0.0	0.0
14	0.0	0.0	0.0	0.0	0.0	0.0	0.0	0.0	0.0	0.0	0.0	0.0
15	1025.2	1021.2	1024.6	1028.4	1023.8	1044.8	1085.8	1144.9	1180.6	1225.5	1223.1	1216.6
16	0.0	0.0	0.0	0.0	0.0	0.0	0.0	0.0	0.0	0.0	0.0	0.0
17	0.0	0.0	0.0	0.0	0.0	0.0	0.0	0.0	0.0	0.0	0.0	0.0
18	0.0	0.0	0.0	0.0	0.0	0.0	0.0	0.0	0.0	0.0	0.0	0.0
19	0.0	0.0	0.0	0.0	0.0	0.0	0.0	0.0	0.0	0.0	0.0	0.0
20	277.6	276.7	278.7	311.3	310.4	296.0	309.3	280.5	276.2	272.4	271.8	264.9
21	78.2	76.6	76.7	76.7	87.2	121.0	169.0	195.0	205.3	221.1	215.7	216.5
22	280.9	283.9	288.8	283.7	281.8	308.0	310.7	309.3	310.7	306.5	308.6	314.5
23	0.0	0.0	0.0	0.0	0.0	0.0	0.0	0.0	0.0	0.0	0.0	0.0
24	18.0	18.5	20.1	20.6	19.4	19.5	22.9	28.0	33.0	36.9	39.3	39.7
25	0.0	0.0	0.0	0.0	0.0	0.0	0.0	0.0	0.0	0.0	0.0	0.0
26	119.6	116.5	115.8	114.8	114.2	118.7	163.5	206.6	239.9	256.2	269.6	280.5
27	0.0	0.0	0.0	0.0	0.0	0.0	0.0	0.0	0.0	0.0	0.0	0.0
28	187.8	187.4	186.3	183.9	195.1	213.4	240.5	263.7	295.4	316.5	323.8	330.6
29	0.0	0.0	0.0	0.0	0.0	0.0	0.0	0.0	0.0	0.0	0.0	0.0
30	74.8	80.2	84.7	79.0	78.1	88.2	90.4	111.4	138.0	143.6	140.0	147.4
31	0.0	0.0	0.0	0.0	0.0	0.0	0.0	0.0	0.0	0.0	0.0	0.0
32	142.4	141.8	137.9	140.8	139.5	139.9	191.4	287.9	334.8	353.3	354.9	363.4
33	0.0	0.0	0.0	0.0	0.0	0.0	0.0	0.0	0.0	0.0	0.0	0.0
34	173.1	173.1	172.8	173.7	188.3	214.5	329.5	409.5	460.2	503.0	489.0	485.7
35	0.0	0.0	0.0	0.0	0.0	0.0	0.0	0.0	0.0	0.0	0.0	0.0
36	72.7	72.0	75.1	72.6	72.9	84.7	120.4	139.5	158.6	162.9	166.6	160.1
37	0.0	0.0	0.0	0.0	0.0	0.0	0.0	0.0	0.0	0.0	0.0	0.0
38	0.0	0.0	0.0	0.0	0.0	0.0	0.0	0.0	0.0	0.0	0.0	0.0
39	0.0	0.0	0.0	0.0	0.0	0.0	0.0	0.0	0.0	0.0	0.0	0.0
40	16.4	16.4	16.4	16.4	16.4	16.4	16.4	16.4	16.4	16.4	16.4	16.4
41	0.0	0.0	0.0	0.0	0.0	0.0	0.0	0.0	0.0	0.0	0.0	0.0

Figure A.1: Load data for all buses in Chalmers grid 17/3-2016

Hour Bus Nr	13	14	15	16	17	18	19	20	21	22	23	24
1	0.0	0.0	0.0	0.0	0.0	0.0	0.0	0.0	0.0	0.0	0.0	0.0
2	866.3	866.7	877.8	869.7	838.8	804.0	755.5	724.6	698.2	669.3	644.4	623.8
3	0.0	0.0	0.0	0.0	0.0	0.0	0.0	0.0	0.0	0.0	0.0	0.0
4	288.8	288.9	292.6	289.9	279.6	268.0	251.8	241.5	232.7	223.1	214.8	207.9
5	0.0	0.0	0.0	0.0	0.0	0.0	0.0	0.0	0.0	0.0	0.0	0.0
6	0.0	0.0	0.0	0.0	0.0	0.0	0.0	0.0	0.0	0.0	0.0	0.0
7	121.3	122.6	122.1	120.9	121.1	109.1	106.4	103.9	103.9	103.8	103.6	103.6
8	0.0	0.0	0.0	0.0	0.0	0.0	0.0	0.0	0.0	0.0	0.0	0.0
9	249.1	255.9	241.9	236.2	208.0	205.5	186.2	142.5	138.5	138.2	138.2	138.2
10	0.0	0.0	0.0	0.0	0.0	0.0	0.0	0.0	0.0	0.0	0.0	0.0
11	44.1	44.0	42.8	39.5	32.2	18.3	12.1	10.9	10.5	10.3	10.3	10.4
12	0.0	0.0	0.0	0.0	0.0	0.0	0.0	0.0	0.0	0.0	0.0	0.0
13	0.0	0.0	0.0	0.0	0.0	0.0	0.0	0.0	0.0	0.0	0.0	0.0
14	0.0	0.0	0.0	0.0	0.0	0.0	0.0	0.0	0.0	0.0	0.0	0.0
15	1215.7	1257.4	1235.2	1211.7	1161.8	1105.6	1062.7	1052.0	1025.8	1028.6	1026.6	1019.6
16	0.0	0.0	0.0	0.0	0.0	0.0	0.0	0.0	0.0	0.0	0.0	0.0
17	0.0	0.0	0.0	0.0	0.0	0.0	0.0	0.0	0.0	0.0	0.0	0.0
18	0.0	0.0	0.0	0.0	0.0	0.0	0.0	0.0	0.0	0.0	0.0	0.0
19	0.0	0.0	0.0	0.0	0.0	0.0	0.0	0.0	0.0	0.0	0.0	0.0
20	267.8	271.3	276.2	288.8	271.8	269.8	275.6	275.6	276.4	276.7	276.7	276.4
21	224.6	225.0	210.5	197.3	143.6	118.1	126.7	110.7	102.0	89.8	83.5	80.4
22	313.1	306.1	313.0	304.2	302.1	295.4	280.7	277.7	277.7	280.2	278.4	280.5
23	0.0	0.0	0.0	0.0	0.0	0.0	0.0	0.0	0.0	0.0	0.0	0.0
24	36.9	38.1	39.3	38.8	33.0	22.6	19.6	19.2	18.4	17.8	17.6	18.0
25	0.0	0.0	0.0	0.0	0.0	0.0	0.0	0.0	0.0	0.0	0.0	0.0
26	264.3	255.6	264.1	266.3	245.9	221.6	204.8	187.1	174.8	165.2	154.3	126.4
27	0.0	0.0	0.0	0.0	0.0	0.0	0.0	0.0	0.0	0.0	0.0	0.0
28	323.9	323.4	326.1	328.2	289.2	248.0	219.6	197.0	184.6	180.2	176.0	170.7
29	0.0	0.0	0.0	0.0	0.0	0.0	0.0	0.0	0.0	0.0	0.0	0.0
30	148.1	143.6	146.7	148.6	132.6	127.8	114.5	96.7	89.7	79.8	72.2	74.5
31	0.0	0.0	0.0	0.0	0.0	0.0	0.0	0.0	0.0	0.0	0.0	0.0
32	387.9	383.5	383.0	348.8	286.6	264.5	207.6	175.8	169.7	161.4	144.2	138.7
33	0.0	0.0	0.0	0.0	0.0	0.0	0.0	0.0	0.0	0.0	0.0	0.0
34	523.8	512.8	516.9	438.2	382.4	318.7	262.6	243.0	208.8	199.0	177.9	173.7
35	0.0	0.0	0.0	0.0	0.0	0.0	0.0	0.0	0.0	0.0	0.0	0.0
36	162.7	161.7	157.1	151.1	138.7	131.7	113.0	100.2	91.4	78.1	75.1	74.6
37	0.0	0.0	0.0	0.0	0.0	0.0	0.0	0.0	0.0	0.0	0.0	0.0
38	0.0	0.0	0.0	0.0	0.0	0.0	0.0	0.0	0.0	0.0	0.0	0.0
39	0.0	0.0	0.0	0.0	0.0	0.0	0.0	0.0	0.0	0.0	0.0	0.0
40	16.4	16.4	16.4	16.4	16.4	16.4	16.4	16.4	16.4	16.4	16.4	16.4
41	0.0	0.0	0.0	0.0	0.0	0.0	0.0	0.0	0.0	0.0	0.0	0.0

Figure A.2: Load data for all buses in Chalmers grid 17/3-2016